Wright State University

CORE Scholar

Browse all Theses and Dissertations | Theses and Dissertations

2011

Cervical Spine Biomechanical Behavior and Injury

Mbulelo T. Makola
Wright State University

Follow this and additional works at: https://corescholar.libraries.wright.edu/etd_all

 Part of the Biomedical Engineering and Bioengineering Commons

Repository Citation

Makola, Mbulelo T., "Cervical Spine Biomechanical Behavior and Injury" (2011). *Browse all Theses and Dissertations*. 1067.
https://corescholar.libraries.wright.edu/etd_all/1067

This Thesis is brought to you for free and open access by the Theses and Dissertations at CORE Scholar. It has been accepted for inclusion in Browse all Theses and Dissertations by an authorized administrator of CORE Scholar. For more information, please contact library-corescholar@wright.edu.

Cervical Spine Biomechanical Behavior and Injury

A thesis submitted in partial fulfillment
of the requirements for the degree of
Master of Science in Engineering

By

Mbulelo Tendai Makola
B.S., 2009, University of Cincinnati

2011
Wright State University

WRIGHT STATE UNIVERSITY

GRADUATE SCHOOL

August 30, 2011

I HEREBY RECOMMEND THAT THE THESIS PREPARED UNDER MY SUPERVISION BY Mbulelo Tendai Makola ENTITLED Cervical Spine Biomechanical Behavior and Injury BE ACCEPTED IN PARTIAL FULFILLMENT OF THE REQUIREMENTS FOR THE DEGREE OF Master of Science in Engineering

Tarun Goswami, D.Sc.
Thesis Director

Thomas N. Hangartner, Ph.D.,
Chair Department of Biomedical Industrial& Human FactorsEngineering

Committee on
Final Examination

Tarun Goswami, D.Sc.

David B. Reynolds, Ph.D.

Richard T. Laughlin, M.D.

Andrew T. Hsu, Ph.D.
Dean, Graduate School

ABSTRACT

Makola, Mbulelo Makola. M.S.Egr., Department of Biomedical Industrial and Human Factors Engineering, Wright State University, 2011.Cervical Spine Biomechanical Behavior and Injury.

A finite element model of the cervical spine including the C2 through C7 levels was developed in order to study the behavior of the cervical spine region. The model was validated in flexion extension, bending, and rotational load scenarios. The model was found to represent the biomechanical behavior of the cervical spine. The validated cervical spine finite element model was used to study spinal injury and disease processes. The model provided qualitative estimates of load carrying and stress distribution as well as range of motion.

Table of Contents

List of Figures

List of Tables

Acknowledgments

I would like to thank my advisor Dr. Tarun Goswami for giving me the opportunity to complete this work. Dr. Goswami has contributed greatly to my understanding of the field. Under his tutelage I have been able to apply sound scientific, engineering, and research principles and methods to the completion of this work. I am certain I will continue to carry and apply what I have learned from him with me in the future. The completion of this work was in no means due to my efforts alone, so I would also like to thank my colleagues at Wright State University, Isaac Mabe, Susan Heuston, and Daniel Reese for their support and expertise in completing this work.

I would also like to thank my family for their continual support throughout this process. My loving wife Alicia for her support and understanding through the process, my parents, brother, and sister for their continual encouragement and support. I could not have accomplished this without them behind me

Chapter 1 – Introduction

The human spine is one of the most important anatomic and physiologic systems serving various important functions. The spine acts to provide primary stability for the torso and head. The spine also acts to protect the very delicate spinal cord. The spine is made up of three distinct regions each consisting of vertebral bodies, intervertebral discs, ligaments and joint systems. The cervical spine region features the C1 – C7 vertebral levels, the thoracic spine with T1 – T12 vertebral levels, the lumbar spine with L1 – L5 vertebral levels. The spinal column terminates with the sacrum and coccyx. The vertebral column can be seen in Figure 1.

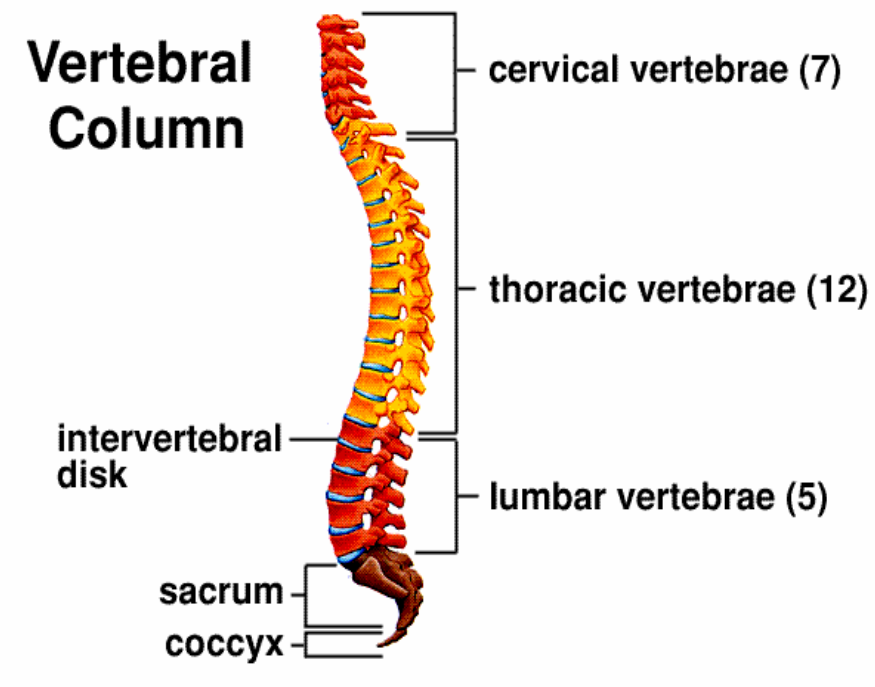

Figure 1.Vertebral Column [1]

The cervical spine offers primary stability to the head neck system along with protecting the spinal cord. The cervical spine features higher levels of motion and flexibility as compared to other regions of the spine. The cervical spine's flexibility leaves it susceptible to a higher rate of injury as compared to the other spinal regions [2]. Cervical spine injuries can occur under traumatic circumstances, or seemingly innocuous circumstances. A fall or motor vehicle accident can lead to the fracture of vertebral bodies and or tearing and bursting of discs and ligaments. A simple of extension of the neck can lead to disc herniation or ligament strains. Spine injury and disease are an important area of continued study. In-vivo studies of the cervical spine

can provide information on the behavior of the spine in non injurious scenarios. In-vivo analyses of the spine cannot provide specific load response information at the vertebral and intervertebral disc levels. In contrast, in-vitro analysis of the cervical spine can provide load displacement response at vertebral segments. In-vitro analyses of the cervical spine are limited to load displacement responses; they cannot provide internal response characteristics such as stress and strain [3,4]. In-vitro cervical spine studies are also limited in their capacity to study spinal injury and disease. Studying spine disease or injury would require the use of injured or diseased cervical spine specimens. Simulating injury using healthy specimens is not ideal as it requires damaging and or destroying the specimens. Finite element (FE) models of the cervical spine can report internal load response characteristics; stress and strain. Models allow for repeatable analyses with multiple scenarios and iterations possible. As such, there has been growing interest and application of FE methods in the study of the cervical spine. Finite element models of the cervical spine have been used to study spine biomechanics, injuries, and response to medical interventions [5-8]. The application of finite element studies of the cervical spine can also be applied to injury risk assessment and mitigation.

The aim of this work is to develop a validated FE model of the cervical spine. The model will be used to study cervical spine biomechanical behavior. This work also aims to study cervical spine disease and injury. A novel approach to quantifying cervical spine injury risk will be developed using the FE model, cervical spine injury risk curves, and dynamicc compressive load scenarios.

Chapter 2 – Literature Review

Development of a finite element model of the spine involves several key areas of consideration. A finite element model of the spine must aim to accurately represent the anatomical features of the spine. Spinal vertebrae, intervertebral discs, ligaments, and their interrelation must all be carefully considered in the development of a model [7,9]. The methods applied in constructing the finite element model play an important role in its ability to accurately represent the cervical spine. The finite element methods applied in analyzing a cervical spine model are also of extreme import [4,8]. In order to gain a better understanding of cervical spine finite element modeling and analysis, a review of the pertinent literature was performed.

2.1 Vertebral Body Modeling

There are two prominent modeling methods in the development of cervical spine vertebral body models. Multi axis digitizers can be used to map points along the vertebral bodies. The resulting set of data points can then be used to create a model via a computer aided drafting (CAD) package. This approach can be applied to the

development of two dimensional (2D) and three dimensional (3D) models [10-13].

For the purposes of finite element analysis, a finite element mesh must be developed. Element selection is of paramount importance in developing any finite element mesh. Element selection is dependent on several factors including, the type of analysis to be performed, and the geometry of the body to be meshed. Cervical spine vertebral bodies can be adequately meshed with 4 noded solid tetrahedral elements; however 8 noded hexahedral elements are considered a better choice [14,15]. Vertebral bodies are made up of two bone regions, the cancellous core and the cortical shell. The cortical shell can be modeled with a separate set of solid or shell elements of distinct thickness, whilst the cancellous core is modeled with solid elements [8]. Though bone is heterogeneous and anisotropic in nature it is generally accepted that homogenous linear elastic material properties can be applied to vertebral body FE models. In addition to vertebral body bone composition, facet joint modeling must also be considered. The facet joints are the joints between posterior regions of the vertebral bodies. They are cartilaginous tissue synovial fluid cores. Facets act to stabilize and constrain the motion of adjacent vertebral bodies. Facet joints do not require the modeling of a geometric component per se, but the computational representation of the kinematic relationship between adjacent vertebras. Facet joints have been modeled with a variety of methods including finite element contact formulations. A summary of methods employed in vertebral body modeling is provided in Table 1.

Table 1.Cervical Spine Vertebral Body Modeling

Author	Year	Source	Cancellous	Cortical	Facet Joints
Yuan et al. [16]	2010	CT	4 node tetrahedral	3 node shell element	N/A
Kallemeyn et al. [9]	2009	CT	8 node hexahedral	8 node hexahedral	Pressure over closure relationship
Panzer et al. [13]		CAD	3D hexahedral	2D quadrilateral	Squeeze film bearing relationship
Esatet al. [17]		CAD	8 node brick	8 node brick	N/A
Galbuseara et al. [18]	2008	CT	8 node hexahedral	8 node hexahedral	Frictionless surface-based contact
Greaves et al. [19]		CT	8 node brick	8 node brick	N/A
Wheeldon et al. [20]		CT	Solid	Solid	Solid / fluid hydraulic incompressible
Teo et al. [15]		CT	Hexahedral Tetrahedral	Hexahedral Tetrahedral	N/A
Ha [21]	2006	CT	20 node brick	8 node shell	Non-linear contact element
Zhang et al. [10]		CAD	8 node brick	8 node brick	Surface to surface contact
Haghpanahi & Mapar [12]		CAD	solid	solid	N/A
Esat et al. [11]		CAD	8 node brick	8 node brick	N/A
Ng et al. [22]	2005	CAD	8 node brick	8 node brick	Nonlinear contact
Brolin et al. [23]	2004	CT	8 node brick	4 node shell	Sliding contact with friction
Ng et al. [24]	2003	CAD	8 node solid	8 node solid	Nonlinear contact
Bozkus et al. [14]	2001	CT	Solid / 4 node tetrahedral		N/A
Teo et al. [25]		CAD		8 node solid	N/A
Graham et al. [26]	2000	CT	tetrahedral	Tetrahedral thin shell	N/A
Kumaresan et al. [27]		CT	8 node brick	8 node brick	8 node, fluid, membrane elements
Zheng et al. [28]		CT	10 node tetrahedral	10 node tetrahedral	N/A

Author	Year	Source	Cancellous	Cortical	Facet Joints
Kumaresan et al. [29]	1999	CT	8 node brick	8 node brick	8 node, fluid, membrane elements
Kumaresan et al. [30]		CT	8 node brick	8 node brick	8 node, fluid, membrane elements
Goel et al. [31]	1998	CT	8 node brick	8 node brick	N/A
Kumaresan et al. [32]		CT	8 node brick	8 node brick	8 node, fluid, membrane elements
Maurel et al. [33]	1997	CAD	8 node	8 node	Gap element
Voo et al. [33]		CT	8 node solid	thin shell	N/A
Yoganandan et al. [4]	1996	CT	8 node solid	thins shell	N/A
Bozic et al. [35]	1994	CT	8 node solid	8 node solid	N/A

Of the 28 studies in the summary table, 9 were modeled using vertebral body data points and a CAD package. The data point modeling approach is limited by the volume of data points. In a 1997 study, Maurel used a set of 154 points to create vertebral body models [33]. More than a decade later in 2009 Panzer created a model using a much larger set of vertebral data points [13]. A comparison of the two models Figure 2 shows a clear difference in model sophistication. The majority of the studies surveyed employ CT scan digitization for model development. In a study by Yoganandan et al., investigators used the program NIH-Image to digitize the CT images and an edge. The data extracted from NIH-Image provided edge locations for the vertebral bodies which were used to create frames of each vertebral body. The frames were then used as the basis for creating the 3D vertebral models using the I-DEAS CAD package [36]. A decade later, a study by Sung Kyu Ha used the Amira image processing software to digitize CT scans, with 3D models and meshes generated in RapidForm and Ansys

respectively [21]. Though the two methods both represent vertebral bodies, the process employed by Ha offered a higher level of model refinement which can be seen in Figure 3.

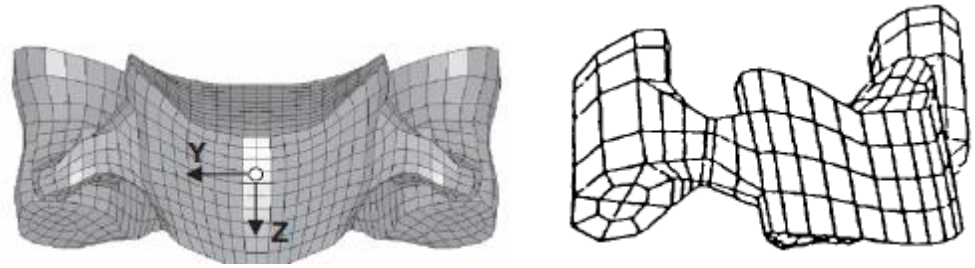

Figure 2. Panzer [13], and Maurel [33], Vertebral Body Models

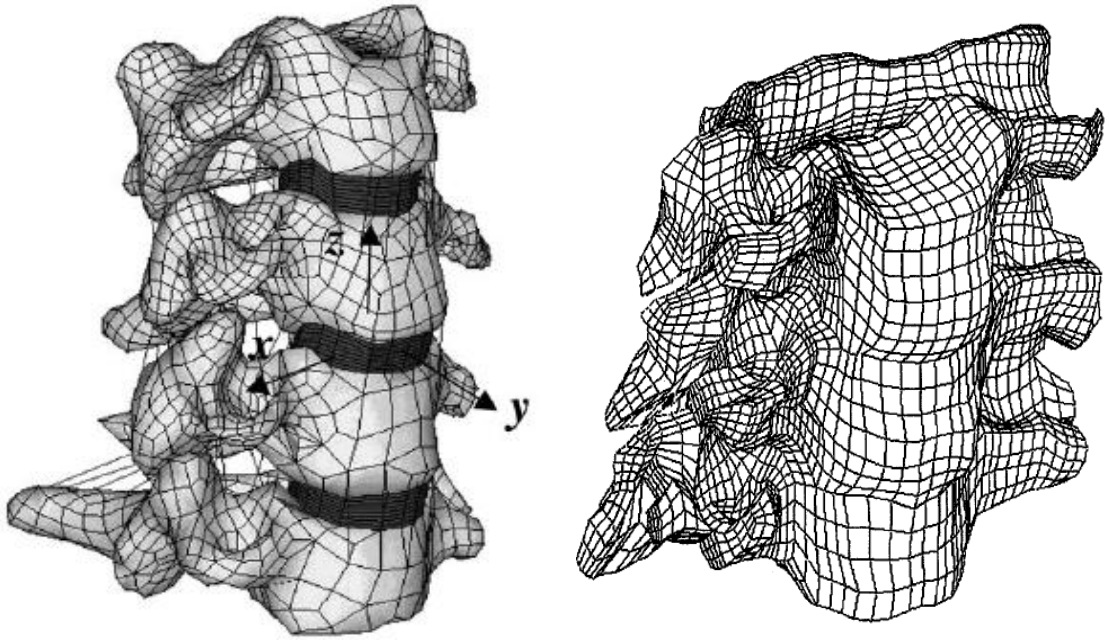

Figure 3. Ha [21], and Yoganandan [36], Vertebral Body Models

The review also yielded a wide variety of methods employed for modeling the facet joints. Some form of contact interaction, nonlinear, frictionless or surface to surface was employed in five of the studies. Four studies modeled facets using 8 noded

membrane elements. The most oft-employed method by far was not modeling the facets at all as evidenced by the 13 studies that used this route the latest being a 2010 study by Li & Lewis [16]. Though the facet joints are important components of the cervical spine it is clear from the modeling approaches employed that omitting them from a finite element is acceptable.

2.2 Intervertebral Discs

Intervertebral discs (IVD) are extremely important to the behavior of the spine. Intervertebral discs act as dampers responding to compressive forces within the spine [8]. Discs are made up of two distinct regions, the outer annulus fibrosus ring, and an inner nucleus pulposus core [21]. The annulus fibrosus functions to resist tension, shear, and torsion. It is made up of collagen fibers embedded in an extracellular matrix composed of water and elastin fibers. Collagen fibers are arranged as a structure of rings throughout the annulus region. Fibers are oriented between 25^{o} and 45^{o} with respect to the horizontal plane. Collagen fibers provide primary stiffness to the annulus region. The gelatinous nucleus pulposus core carries compressive loads. The intervertebral discs interact with adjacent vertebral bodies via cartilaginous endplates [37-39].

Intervertebral disc bodies cannot be modeled directly from spine CT scans because CTs do not capture soft tissue images. Cryomicrotomy of magnetic resonance images (MRI) can be used to fill in the missing soft tissue images [8,34]. An alternative

to employing cryomicrotomy is to model intervertebral discs in reference to their positionin the vertebral body disc spaces [8]. An IVD can be modeled with a CAD package as a cylindrical disc [40]. For finite element analysis purposes the intervertebral disc annulus is often modeled as a fiber reinforced composite. Solid brick elements are reinforced by a fiber or rebar element matrix of alternating angular orientation. The reinforcing fibers often employ a nonlinear response behavior unique to that of the solid annulus elements they are suspended within. The nucleus has been modeled as an incompressible fluid using incompressible fluid elements [41]. There is precedence in the literature to model the cartilaginous disc endplates that interface with the vertebral bodies as a separate shell element component [21]. Figure 4 illustrates the disc modeling approach employed by Ha.

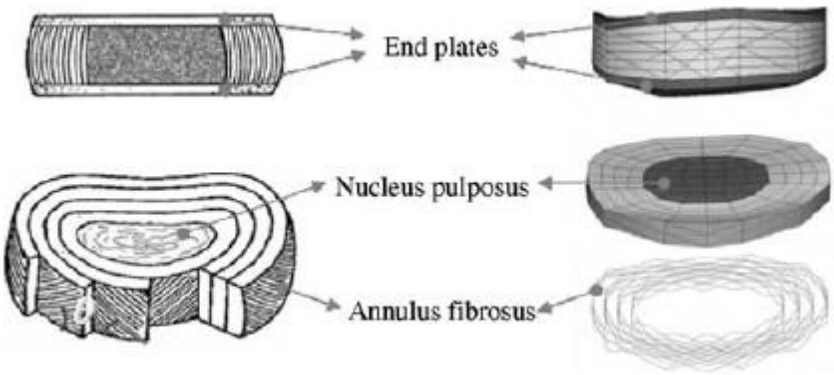

Figure 4. Intervertebral Disc Model [21]

An alternative to modeling the annulus and nucleus involves approximating them as homogenous regions and applying a modulus of elasticity and Poisons ratio. The mixed mode load carrying characteristics of intervertebral discs and their highly

fluid makeup can pose challenges in accurately modeling their behavior. There is precedent for approximating disc behavior with linear isotropic elastic material and constitutive models in order to ease the FE modeling and analysis. There are however studies that aim to better represent disc behavior by employing hyper elastic constitutive models to approximate the nonlinear response of the IVD [42]. Table 2 summarizes some of the methods applied to modeling intervertebral discs.

Table 2. Cervical Spine Intervertebral Body Modeling

Author	Year	Disc Components	Elements	Behavior
Li et al. [16]	2010	Annulus fibrosus Nucleus pulposus	8 node brick 4 node tetrahedral	Isotropic Elastic
Kallemeyn et al. [9]	2009	Annulus fibrosus Nucleus pulposus	8 node tetrahedral Hydrostatic fluid	Isotropic Elastic
Panzer et al. [13]		Annulus fibrosus Nucleus pulposus	Hexahedral element Incompressible element	Orthotropic Elastic Fluid Density
Esatet al. [17]		Annulus fibrosus Nucleus pulposus	8 node brick	Viscoelastic
Galbuseara et al. [18]	2008	Annulus fibrosus Nucleus pulposus	Hexahedral element Tension only truss	Isotropic Elastic
Wheeldon et al. [20]		Annulus fibrosus Nucleus pulposus	Solid element Rebar element Incompressible fluid	Nonlinear Stress Strain Curve Fluid Density
Palomar et al. [42]		Annulus fibrosus Nucleus pulposus	Solid element Linear tetrahedral Incompressible fluid	Hyperelastic Strain Energy Function
Schmidt et al. [43]	2007	Annulus fibrosus Nucleus pulposus	8 node solid element 3D spring element	Hyperelastic
Ha [21]	2006	Annulus fibrosus Nucleus pulposus	20 node solid element Tension only spar	Isotropic Elastic
Zhang et al. [10]		Annulus fibrosus Nucleus pulposus	8 node brick	Isotropic Elastic
Ng et al. [10]	2005	Annulus fibrosus Nucleus pulposus	8 node solid element Fluid element	Isotropic Elastic
Eberlin et al. [41]	2004	Annulus fibrosus Nucleus pulposus	8 & 20 node hexahedral Incompressible fluid	Heterogeneous Isotropic Elastic
Meakin et al. [40]	2001	Annulus Nucleus pulposus	Solid element Fluid element	Isotropic Elastic

Author	Year	Disc Components	Elements	Behavior
Kumaresan et al. [29]	1999	Annulus fibrosus Nucleus pulposus	8 node solid Rebar element Incompressible fluid	Isotropic Elastic
Maurel et al. [33]	1997	Annulus fibrosus	8 node element Cable element	Isotropic Elastic
Voo et al. [34]		Uniform disc	8 node element	Isotropic Elastic
Yoganandan et al. [44]	1996	Uniform disc	8 node element	Isotropic Elastic
Bozic et al. [35]	1994	Uniform disc	Springs element	Isotropic Elastic

Of the 19 studies included in the summary table, 13 employed linear isotropic elastic constitutive models. This high uptake of linear approximation techniques somewhat validates the approach. Of the five studies that did not assume linear disc behavior, Palomar et al. developed novel constitutive models of the disc annulus and nucleus. The authors used in-vitro data sourced from a specific analysis of the tensile behavior of multiple layers of annulus under very slow strain rates performed by Ebara et al. [45]. The data was used to adjust material properties of a strain energy function developed for specifically for annulus fibers by co collaborators Holzapfel et al. [46]. The constitutive model was then implemented via a UMAT user subroutine in the Abaqus finite element software package. The disc nucleus was modeled using an incompressible hyperelastic constitutive model. The model parameters were derived by extrapolating previously accepted elastic parameters into the hyperelastic domain. The model allowed for greater understanding of internal stress response of the intervertebral discs [42]. One study, by Esat and Acar employed a viscoelastic model to approximate disc behavior [17]. The viscoelastic approach offers a better representation of the nonlinear response characteristics of the disc and also poses

somewhat less computational demands as compared to a hyperelastic constitutive model.

2.3 Ligaments

Ligaments are the supportive connective structures of the spine. Ligaments of the spine include the ligamentumflavum (LF), interspinous ligament (ISL), capsular ligament (CL) and intertransverse (ITL) ligaments. The intertransverse set of ligaments function to support individual vertebra. The anterior longitudinal (ALL), posterior longitudinal (PLL), and the supraspinous ligament (SSL) act as supports for series of vertebra [8]. Spinal ligaments are often modeled based on knowledge of their anatomical makeup, locations, and relation to vertebra and intervertebral discs. Figures 5 and 6 illustrate some ligament modeling approaches.

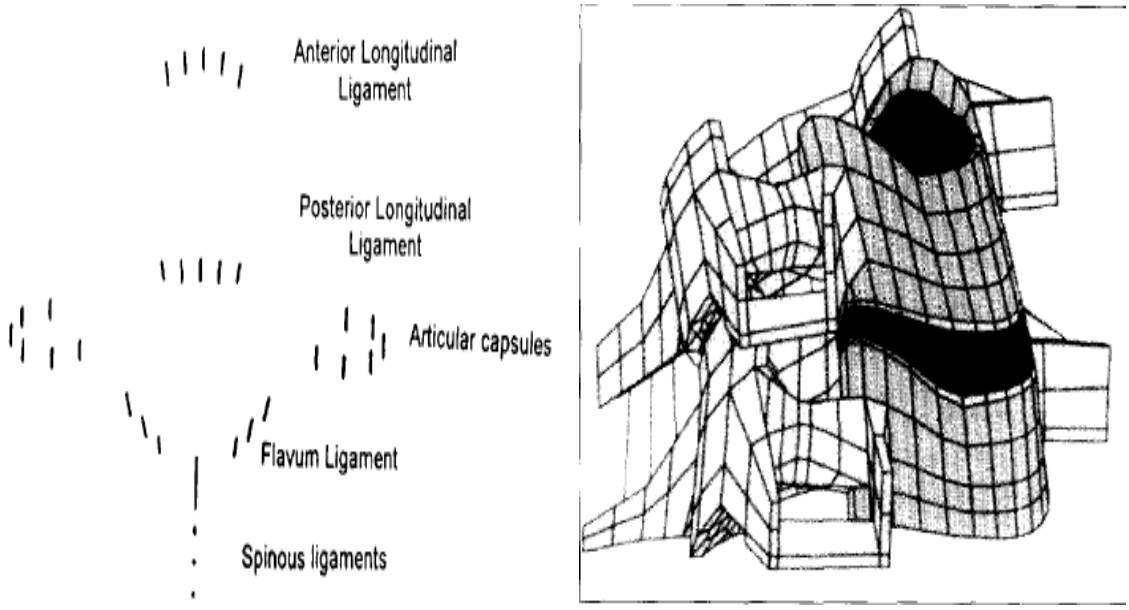

Figure 5. Cervical Spinal Ligament Models [33]

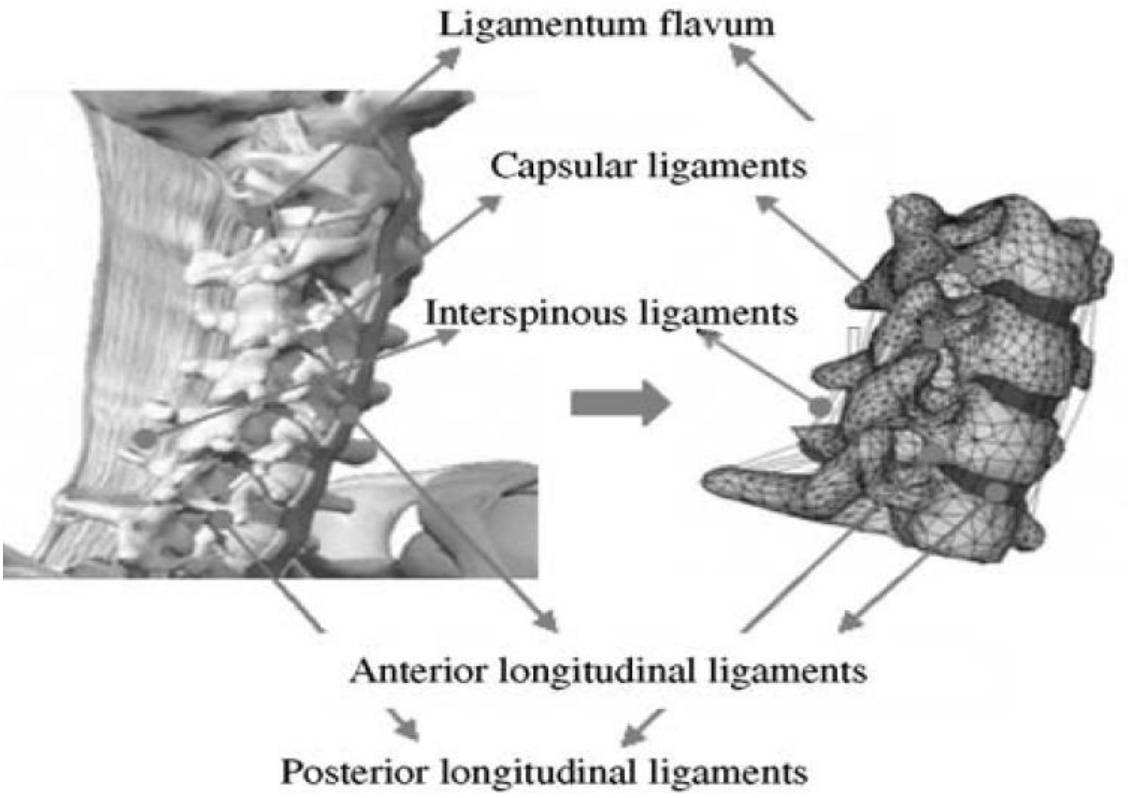

Figure 6. Cervical Spine Ligaments & FE Model [21]

Both the Maurel and Ha ligament modeling approaches aimed to map intervertebral disc locations to the FSU models. The studies were separated by a period of about ten years which is somewhat evident in the level of sophistication between the two. In-vitro studies provide ligament cross sectional area, length, and kinematic behavior [47]. Spring, cable, truss, and tension only elements have all been employed in the modeling of ligaments.Ligaments are most often modeled using non linear tension only constitutive models [8]. A summary of some ligament modeling techniques applied is provided in Table 3.

Table 3. Cervical Spine Ligament Modeling

Author	Year	Ligaments	Elements	Behavior
Li et al. [16]	2010	ALL, PLL, CL, LF, ISL, TL, APL	Tension-only spar	Nonlinear
Kallemeyn et al. [9]	2009	ALL, PLL, CL, LF, ISL	2 node truss	Nonlinear
Panzer et al. [13]		ALL, PLL, CL, LF, ISL	1D tension only	Nonlinear
Galbuseara et al. [18]	2008	ALL, PLL, CL, LF, ISL	Spring element	Force Deflection Curve
Greaves et al. [19]		ALL, PLL, CL, LF, ISL	2 node link	Nonlinear
Palomar et al. [42]		ALL, PLL, YL, ISL, ITL	Tension only truss	Nonlinear
Wheeldon et al. [20]		ALL, PLL, LF, CL, ISL	Spring element	Force Deflection Curve
Schmidt et al. [43]	2007	ALL, PLL, CL, LF, ISL, SSL	Spring element	Force Deflection Curve
Ha [21]	2006	ALL, PLL, LF, ISL, CL	Tension only spar	Linear
Zhang et al. [10]		ALL, PLL, SSL, ISl, LF, CL, AL, TL, NL, APL	2 node link	Linear
Ng et al. [22]	2005	ALL, PLL, LF, ISL, CL	Tension only cable	Nonlinear
Brolin et al. [23]	2004	ALL, PLL, TL, LF, CL, ISL	Tension only spring	Force Deflection Curve
Eberlin et al. [41]		ALL, PLL, TL, LF, CL, ISL	Membrane element	Nonlinear
Kumaresan et al. [27]	2000	ALL, PLL, CL, LF, ISL	Tension only element	Force Deflection Curve
Kumaresan et al. [30]	1999	ALL, PLL, CL, LF, ISL	Tension only element	Force Deflection Curve
Maurel et al. [33]	1997	ALL, PLL, CL, Lf, ISl, SSL	Tension only cable element	Linear
Voo et al. [34]		ALL, PLL, CL, LF, ISL	2 node uniaxial	Linear

The summary table clearly illustrates that despite the difficulties of visualizing spinal ligaments for modeling purposes; they are still included in most cervical spine finite element models. It is also evident that the majority of investigators aim to capture the nonlinear behavior of cervical spine ligaments. The degree to which ligament nonlinearity has been captured does vary amongst studies. The use of finite elements with nonlinear characteristics has been applied and deemed adequate to represent ligament non linearity [21]. Strain dependent modulli of elasticities also

provide nonlinear response characteristics. Strain dependent moduli of elasticity are often sourced from in vitro experimentation of cervical spine segments [9,47]. Force deflection curves sourced from in-vitro experiments can provide data for nonlinear constitutive models [18,20]. It is clear from a review of the literature that investigators are continually developing and applying sophisticated modeling techniques to spinal ligaments.

2.4 Biomechanical & Injury Analysis

Mathematical modeling approaches allow for both static and dynamic analysis of the cervical spine. Dynamic analyses of the spine often aim to characterize the response of the cervical region during an impact with the goal of better understanding vehicular injury scenarios such as whiplash. Dynamic models of the cervical spine often include the entire cervical spine, and the head. Vertebral bodies have been modeled as rigid bodies, with soft tissues such as spinal ligaments represented by linear springs [11,48-50]. This modeling approach somewhat limits the load response data that can be derived for specific vertebral bodies and intervertebral discs.

Static FE analyses focus on analysis of load response characteristics of cervical spine segments. In an effort to represent the load response as accurately as possible, static FE models are constructed with as much detail as possible [9,13,21,31]. In contrast to dynamic models, static models often focus on two to three vertebral bodies as opposed to the complete cervical spine. These functional spinal units (FSU) can provide important internal load and segment displacement data [24]. Static analyses also allow for corroboration of FE results with in vitro study load displacement results. Static analyses have been used to analyze a variety of topics including spinal column biomechanics, soft tissue effects on behavior, soft and hard tissue injuries, and even prosthetic disc replacements [10,18,21,34,51].

Cervical spine biomechanics includes but is not limited to the study of the range of motion (ROM) of the spine. The cervical spine exhibits higher degrees of flexion, extension, and rotation as compared to the lumbar and thoracic spine regions. By quantifying the ROM in each mode a better understanding of how the spine behaves during activities of daily living (ADL) is gained. An understanding of ROM under ADL can lead to a better understanding of cervical spine injuries. An FE analysis can reveal scenarios in which spine ROM is violated leading to possible injury to soft tissues, in fact, stress and strain rates within ligaments and intervertebral discs can be estimated, and corroborated with potential injury [8]. ROM values vary greatly depending on the cervical spine level considered, the loads applied and the specific study. For example the C3-C4 level has exhibited from about 2^{o} to 4^{o} in extension across a couple of in-vitro studies [52,53]. A more direct approach can be approached to analyzing spine injury via FEA in which a specific injury scenario applied to the model. Bozkus et al. studied the Jefferson Fracture by applying pure axial loads that are often experienced in Jefferson Fractures [14]. As stated, static finite element model analyses lend themselves well to validation of cervical spine finite element models. Validation of any finite element model is an extremely important process that confirms that the model and assumptions there in adequately represent the behavior of the spine. There have been in-vitro studies of the cervical spine and spine segments that can act as comparison and validation cases for finite element studies [53-55]. In order to use an in-vitro study as a comparison case, test conditions including loading and constraints must aim for

equivalency. It is accepted that an FE analysis cannot exactly replicate an in-vitro study as there are clear differences in load application methods, equipment, and the actual spine specimens. Richter et al. performed a load displacement study of the cervical spine using a novel spinal load simulator they had previously developed; the system can be seen in Figure 6 [55,56].

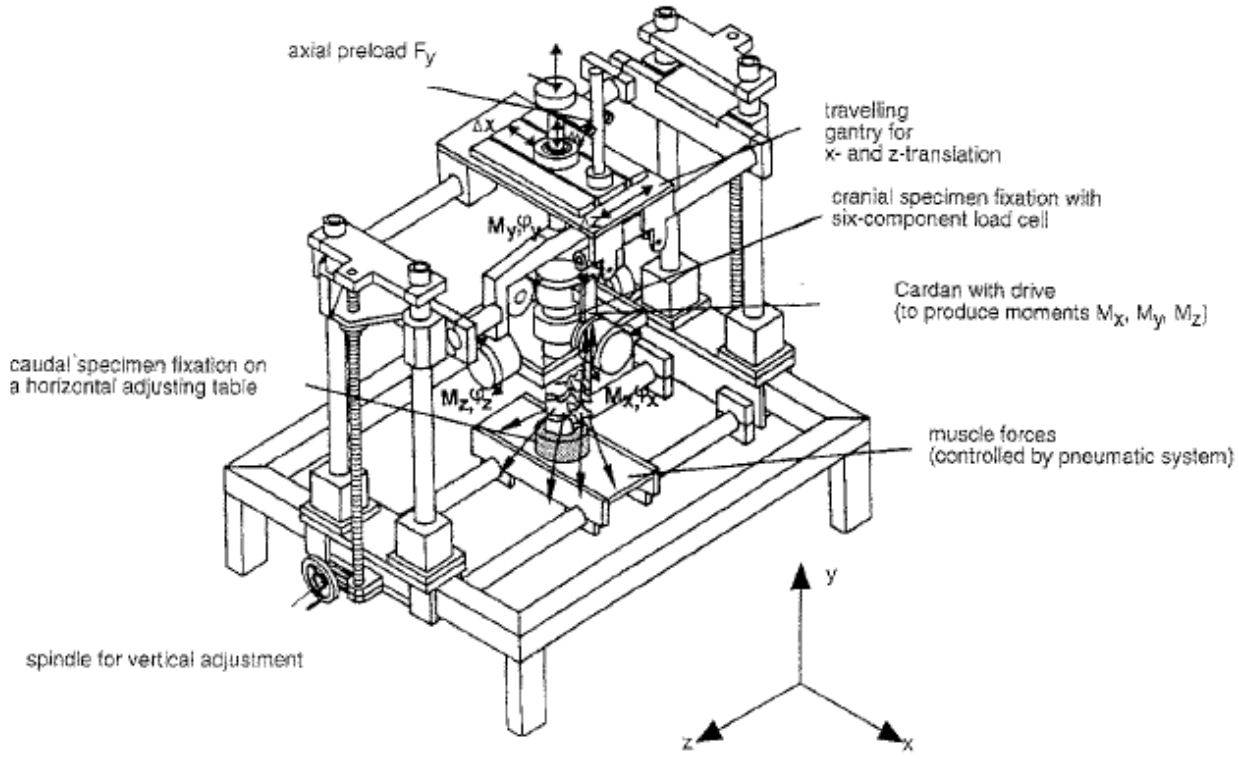

Figure 7. In-vitro Spine Tester [56]

Along with the test rig pictured, the Richter in-vitro testing system includes an ultrasound motion analysis system and all the germane computing and data acquisition tools. This brief survey of the tools and methods employed in just one in-vitro spine study helps to shed light on some of the impetus for developing better FEA methods and

models of the spine. Despite the differences, in-vitro studies still provide invaluable validation data to spine FE studies. Additionally, the differences do not limit the load cases applied to finite element studies to those already employed in-vitro. By verifying a study under known in-vitro conditions investigators can assume the response of the finite element model is valid within a certain range of displacements and continue to test different scenarios [7,24]. The following summary table provides study types, load conditions and validation methods employed.

Table 4. Cervical Spine Finite Element Studies

Author	Year	Study Type	Spine Levels	Spine Levels	BC	Validation
Li et al. [16]	2010	Static Surgery	All Segment	0.33 - 2 Nm Flexion Extension Lateral Bending Axial Rotation 1 Nm + 73.6 Compression	Inferior Endplate Fully Fixed	Panjabi et al. 2001; Wheeldon et al. 2006
Kallemeyn et al. [9]	2009	Static Biomechanics	2 Segment	1 Nm Flexion Extension Lateral Bending Axial Rotation + 73.6 N Compression 600 N Compression	Inferior Endplate Fully Fixed	Moroney et al. 1988; Traynelis et al. 1993; Pintar et al. 1995
Panzer et al. [13]		Static Biomechanics	2 Segment	0.3 – 3.5 Nm Flexion Extension Lateral Bending Axial Rotation	Inferior Endplate Fully Fixed	Goel et al. 1988; Panjabi et al. 2001; Camacho et al. 1997; Wheeldon et al. 2006; Nightingale et al. 2007
Esat et al. [17]		Static Dynamic Biomechanics	3 Segment	1.6 Nm Flexion Extension 73.6 N Compression Frontal/Rear Impact Dynamic Load Curve	Inferior Endplate Fully Fixed	Teo and Ng, 2001
Galbuseara et al. [18]	2008	Static Prosthesis	4 Segment	2.5 Nm Flexion Extension 100 N Compression	Inferior Endplate Fully Fixed	Wheeldon et al. 2006
Greaves et al. [19]		Static Injury	3 Segment	Injury based deflection	Injury based	In-vivo Hung et al. 1979; Maiman et al. 1989

Author	Year	Study Type	Spine Levels	Spine Levels	BC	Validation
Wheeldon et al. [20]		Static Biomechanics	4 Segment	0 – 2 Nm Flexion Extension Axial Rotation	Inferior Endplate Fully Fixed	Gilad & Nissan 1986 Panjabi et al. 1991
Teo et al. [15]		Static Mesh Generation	7 Segment	N/A	Inferior Endplate Fully Fixed	N/A
Ha [21]	2006	Static Prosthesis	4 Segment	1 Nm Flexion Extension Lateral Bending Axial Rotation	Inferior Endplate Fully Fixed	Moroney et al. 1991; Pelker et al. 1987; Goel et al. 1998; Teo& Ng et al. 2001
Zhang et al. [10]		Static Biomechanics	8 Segment	1 Nm Flexion Extension Lateral Bending Axial Rotation 50 N Compression	Inferior Endplate Fully Fixed	Goel et al. 1984; Moroney et al. 1988; Goel& Clausen 1998; Panjabi et al. 2001
Haghpanahi & Mapar [12]		Static Biomechanics	5 Segment	1.8 Nm Flexion Extension	Inferior Endplate Fully Fixed	Lopez-Espinea (FEA) 2004; Goel et al. 1984; Voo et al. 1997; Maurel et al. 1997 Moroney et al. 1988
Esat et al. [11]	2005	Static Dynamic Biomechanics	3 Segment	1.6 Nm Flexion Extension 73.6 N Compression Frontal/Rear Impact Dynamic Load Curve	Inferior Endplate Fully Fixed	Shea et al. 1991
Ng et al. [22]		Static Injury	6 Segment	1.5 Nm Flexion Extension	Inferior Endplate Fully Fixed	Panjabi et al. 1986; Moroney et al. 1988; Schulte et al. 1989; Pelker et al. 1991

Author	Year	Study Type	Spine Levels	Spine Levels	BC	Validation
Brolin et al. [23]	2004	Static Biomechanics	2 Segment	1.5, 10 Nm Flexion Extension BendingRotation 1500 N Tension	Inferior Endplate Fully Fixed	Panjabi et al. 1991; Panjabi et al. 1991; Van et al.2000; Goel et al. 1990
Ng et al. [24]	2003	Static Injury	3 Segment	1.8 Nm Flexion Extension Lateral Bending Axial Rotation 73.6 N Compression	Inferior Endplate Fully Fixed	Shea et al. 1991 Moroney et al. 1988 Pelker et al. 1991 Maurel et al. 1997 Goel et al. 1998
Bozkus et al. [57]	2001	Static Injury	1 Segment	200 – 1200 N Compression	Inferior Endplate Fully Fixed	Cadaver Study
Teo et al. [25]		Static Biomechanics	3 Segment	1 mm Axial Displacement	Inferior Endplate Fully Fixed	Shea et al. 1991; Yoganandan et al. 1996 (FEA)
Graham et al. [26]	2000	Static Injury	1 Segment	1279, 1736 N Compression	Inferior Endplate Fully Fixed	Doherty et al 1993
Kumaresan et al. [27]		Static Biomechanics	3 Segment	0.5 Nm Flexion Extension 200 N Compression	Inferior Endplate Fully Fixed	FEA Kumaresan et al. 1997
Zheng et al. [28]		Static Surgery	5 Segment	196 N Compression	Injury Case Dependent	N/A
Kumaresan et al. [29]	1999	Static Biomechanics	3 Segment	0.5 – 1.8 Nm Flexion Extension Lateral Bending Axial Rotation	Inferior Endplate Fully Fixed	Cadaver Study Pintar et al. 1995
Kumaresan et al. [30]		Static Biomechanics	3 Segment	1.8 Nm Flexion Extension Lateral Bending Axial Rotation Compression	Inferior Endplate Fully Fixed	Moroney et al. 1988

Author	Year	Study Type	Spine Levels	Spine Levels	BC	Validation
Goel et al. [31]	1998	Static Biomechanics	2 Segment	1.8 Nm Flexion Extension Lateral Bending Axial Rotation 73.5 N Compression	Inferior Endplate Fully Fixed	Moroney et al. 1988 Clausen et al. 1996 Goel et al. 1988 Teo et al. (FEA) 1994
Kumaresan et al. [32]		Static Biomechanics	2 Segment	Flexion Extension Lateral Bending Compression	Inferior Endplate Fully Fixed	N/A
Maurel et al. [33]	1997	Static Biomechanics	5 Segment	0 – 1.6 Nm Flexion Extension Lateral Bending Axial Rotation 6 N Compression	Inferior Endplate Fully Fixed	Cressend 1992; Panjabi et al. 1986; Wen et al. 1993; Moroney et al. 1984, 1998
Voo et al. [34]		Static Surgery	3 Segment	1.8 Nm Flexion Extension Lateral Bending Axial Rotation	Inferior Endplate Fully Fixed	Liu et al. 1982; Moroney et al. 1988
Yoganandan et al. [44]	1996	Static Biomechanics	3 Segment	1 mm Compression	Inferior Endplate Fully Fixed	Shea et al. 1991
Bozic et al. [35]	1994	Static Injury	1 Segment	3400 N Compression	Inferior Endplate Fixed by Spring	N/A

The 27 studies included in the summary table spanned a period of about 16 years. At the time, the 1994 study by Bozic et al. was one of the first FE studies focused on the cervical spine region. The study investigated the burst fracture mechanism in cervical vertebral bodies. The investigators applied compressive breaking loads to the vertebral bodies and measured the resulting stress responses [35]. The analysis results seemed to indicate that the vertebra was most susceptible to fracture in its anterior

region. Along with the Bozic et al. study, there were four other studies that investigated cervical spine injury [19,24,26,57]. The most recent study in the summary table, by Li and Lewis, aimed to study the effects of surgical procedures used to treat disc degeneration on the biomechanical properties of the cervical spine. The authors created and validated an FE model of segments C1-C7 using CT scan data, the medical imaging software packages Mimics, and RapidForm, the CAD package ProEngineer, and the finite element package Abaqus. The validated model was then modified to simulate anterior cervical discectomy, percutaneous nucleotomy, and disc nucleus replacement. Each analysis model was then subject to pure bending, and rotation moments, along with combinations of bending and rotation with axial compression. Study findings were that the simulated percutaneous nucleotomy and simulated disc nucleus replacements better maintained the spine biomechanical behavior as compared to the simulated discectomy and fusion models [16]. Comparing the Bozic and Li studies shows some of the changes and advancements in applying FEA to the study of the spine. The study by Bozic featured a single vertebra subject to pure axial loads. Li and Lewis created models of the full cervical spinal column and subject them to compressive loads, and bending moments.

A similar study to Li and Lewis by Sung Kyu Ha employed a finite element model of the cervical spine to study the effects of spinal fusion and the implantation of a prosthetic disc on spine behavior [21]. Spinal fusion was modeled by applying a graft with the material properties of cortical bone between adjacent vertebral segments. The

disc prosthesis was modeled by replacing the entire intervertebral disc with an elastomer core. Efforts were made to select an elastomer core with similar properties to that of the intervertebral disc. The analysis results showed that spinal fusion led to a 50 – 70% reduction in ROM for the fused spinal segment. The analysis also showed the introduction of a prosthetic disc did not change the range of motion seen in the motion segment [21]. Using a validated finite element model of the cervical spine, the study was able to help predict the effect of two interventions that are often employed in spinal injury cases.

All but two of the studies were static analyses. The studies, by Esat et al. are unique in the field in that they combine both static and dynamic analysis methods [11,17]. The investigators aimed to simulate the response of the head and neck system under frontal and rear impact scenarios. A multi-body dynamic head and neck model was developed and validated using human volunteer experimental data. The investigators took the analysis further by developing a finite element model of the cervical spine and intervertebral discs. The finite element model was then used to study the response of the intervertebral discs to the dynamic impact loads. A key difference between the two studies is the 2009 study employed a viscoelastic model for the intervertebral disc model. The viscoelastic model based on in-vitro relaxation testing provided a better representation of the discs load response behavior as compared to the linear elastic approximation employed in the earlier study. Both studies found that

the disc annulus region carries higher levels of stress as compared to the disc nucleus [11].

2.5 Summary

FEA has clearly emerged as a method for studying the cervical spine. Vertebral body modeling methods have improved with the emergence of medical imaging software and improved computational models. Vertebral body fracture stresses can now be simulated via FEA with results closely matching in-vitro experiments. Cervical intervertebral disc modeling has also continued to improve with disc nonlinearity captured via complex multi factor computational models. FE modeling of nonlinearity has also improved for cervical spine ligaments. Ligament models can now accurately reproduce in-vitro load displacement and strain characteristics. The developments in modeling of cervical spine component FE models has allowed for FE FSUs that accurately represent static biomechanical behavior as compared to in-vitro experiments. Across the studies surveyed FE model ROM consistently fell within a standard deviation of in-vitro experimentation. FE studies have also captured effects of spine interventions such as fusion and disc replacement with reduction in ROM of at minimum 50 – 70% corroborated in-vitro. With continued development cervical spine FE models and analysis will be able to better represent the cervical spine in-vivo providing a powerful tool for better understanding of spine biomechanical and kinematic behavior and injury mechanisms.

Chapter 3 – Materials and Methods

The review of the literature carried out provided a strong base for developing a finite element model of the cervical spine. Some of the common approaches, assumptions, and limitations in modeling methods were identified. The review also highlighted areas of potential improvement and development.

3.1 Vertebral Body Model Development

As discussed in the introduction, a key area of consideration in developing finite element model of the cervical spine is the actual basis of the vertebral body models. The two prominent approaches are using a 3D digitizer to create a set of data points and coordinates with which the vertebrae will be modeled in a CAD package. The second approach involves using CT scans and some sort of edge detection program or medical imaging software to create the vertebral model. Each approach offers unique advantages and disadvantages. The current study uses cervical spine CT scans and the medical imaging software Mimics by Materialize Lueven, Belgium.to develop vertebral models. The CT scans were obtained from the Miami Valley Hospital in accordance with the "Risk Assessment of Cervical Spine Injuries" IRB protocol 10-0011. The cervical spine model in the current study is based on the CT scans of an 18 – 40 year old males.

The CT scans were imported into the Mimics medical imaging software. Mimics allows for the partitioning of CT scans based on apparent bone density. This automatic thresholding allows for the isolation of the vertebral column. The vertebral column partition can then be further refined and isolated into individual vertebra.Mimics also has the capability to create a finite element mesh of the 3D models. This workflow is illustrated in Figures 8.

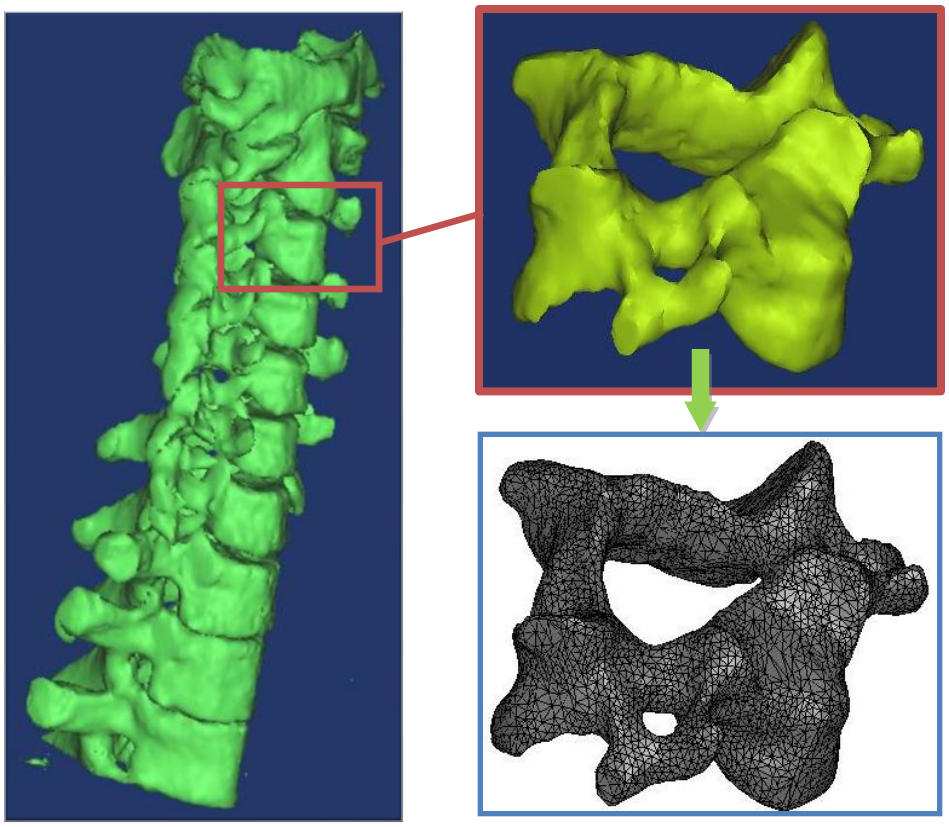

Figure 8. Mimics Cervical Spine Model and Mesh

After each vertebral body, levels C2 – C7, was meshed, the segments were exported from Mimics into the Abaqus finite element software package. One of the most important considerations in any finite element analysis is the makeup of the finite element mesh. A mesh made up of hexahedral elements is considered ideal. However, hexahedral elements are somewhat limited in their ability to accurately represent the geometry of vertebral bodies. As such, Mimics develops a 4 node tetrahedral element mesh for the vertebral body models. Once the mesh has been imported into Abaqus, further checks can be made regarding its validity and quality.

The next step in the vertebral body modeling process involved assigning material properties and constitutive models. The vertebral bodies are made up of two distinct bone regions, the cancellous core and the cancellous core. The cortical shell has been modeled via a layer of shell tetrahedral elements with constant uniform thickness offset from the cortical shell. This approach does not fully represent the natural bony anisotropy; however the method has been employed in the literature and is an acceptable approximation [4]. After defining the cancellous and cortical bone regions the posterior elements including pedicles and cervical lamina were defined. It was decided that the facet and uncinate joints would not be considered in this cervical spine finite element model. Precedence for this modeling approach has been clearly established in the literature [4,11,12,14-17,19,25,26,28,31,34,35]. The material properties sourced from the literature andelement information for the vertebral bodies are presented in Table 4 and 5 [9].

Table 5. Vertebral Body Material Properties [9]

Vertebral Region	Element Type	Material Property
Cancellous Core	4 node tetrahedral	E = 450 MPa, ν = 0.25, ρ = 1.1e-6 kg/mm^3
Cortical Shell	3 node shell	E = 10000 MPa, ν = 0.3, ρ = 1.7e-6 kg/mm^3
Posterior Bone	4 node tetrahedral	E = 3500 MPa, ν = 0.25, ρ = 1.4e-6 kg/mm^3

3.2 Intervertebral Disc Model Development

Unlike the vertebral bodies that can be modeled directly from CT scans, the intervertebral discs and other soft tissue do not register in CT scans and cannot be automatically modeled. There are two predominant approaches to model

intervertebral discs in light of this shortfall. MRI or cryomicrotomy imaging can be used to image the discs. The alternative approach is to model the intervertebral discs in a CAD package by interpolating between the adjacent vertebral levels. This was the approach employed in the current study. The procedure employed within Abaqus allowed the superior and inferior disc surfaces to directly match, and mate to the adjacent vertebral bodies.

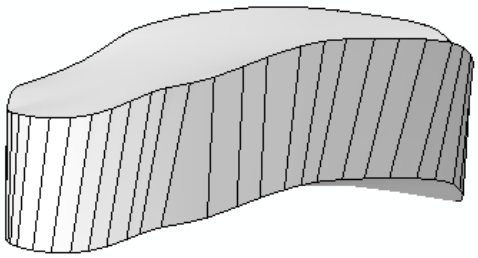

Figure 9. Disc 3-4 Model

The intervertebral discs are made up of two major regions, the annulus fibrosus and nucleus pulposus. The annulus fibrosus was modeled as a homogeneous linear elastic annulus ground region with embedded fibrous reinforcement [21]. The annulus ground was modeled via solid tetrahedral elements. The annulus fibers were modeled alternating at 25^{o} angles via shell and rebar elements. The disc nucleus was modeled as homogeneous linear elastic with four noded tetrahedral elements. It was decided that a linear isotropic elastic constitutive model would be employed in modeling the intervertebral disc regions. The material property values applied to each region were sourced from the literature [9,58] and have been provided in Table 6.

Table 6. Intervertebral Discs [9,58]

Disc Region	Element Type	Material Property
Nucleus Pulposus	4 node tetrahedral	E = 3.4 MPa, ν = 0.49, ρ = 1.02e-6 kg/mm^3
Annulus Ground	4 node tetrahedral	E = 4.2 MPa, ν = 0.45, ρ = 1.05e-6 kg/mm^3
Annulus Fibers	Rebar	E = 450 MPa, ν = 0.3, ρ = 1.0e-6 kg/mm^3

3.3 Ligament Model Development

The cervical ligaments, similar to the intervertebral discs, were modeled by interpolating their position relative to the adjacent vertebral levels. Ligament positions are based on their anatomical positions and in-vitro studies. Linear elastic constitutive models based on an in-vitro study of ligament characteristics were applied to the ligament discs [47]. Ligament details can be seen in Table 7.

Table 7. Cervical Spine Ligaments [47]

Ligament	Element Type	Area (mm^2)	Material Property
C2 – C5			
ALL	2node beam	11.1	E = 43.8(<13%)26.3(>13%)MPa, ρ = 1.0e-6 kg/mm^3
PLL	2 node beam	11.3	E = 40.9(<11%)22.2(>11%)MPa, ρ = 1.0e-6 kg/mm^3
CL	2 node beam	42.2	E = 5.0(<57%)3.3(>57%)MPa, ρ = 1.0e-6 kg/mm^3
LF	2 node beam	460	E = 3.1(<41%)2.1(>41%)MPa, ρ = 1.0e-6 kg/mm^3
ISL	2 node beam	13.0	E = 4.9(<26%)3.1(>26%)MPa, ρ = 1.0e-6 kg/mm^3
C5 – C7			
ALL	2node beam	12.1	E = 28.2(<15%) 28.4(>15%)MPa, ρ = 1.0e-6 kg/mm^3
PLL	2 node beam	14.7	E = 23.0(<11%) 24.6(>11%)MPa, ρ = 1.0e-6 kg/mm^3
CL	2 node beam	49.5	E = 4.8(<57%)3.4(>57%)MPa, ρ = 1.0e-6 kg/mm^3
LF	2 node beam	48.9	E = 3.5(<35%) 3.4(>35%)MPa, ρ = 1.0e-6 kg/mm^3
ISL	2 node beam	13.4	E = 5.0(<27%)3.3(>27%)MPa, ρ = 1.0e-6 kg/mm^3

3.4 Model Validation and Biomechanical Behavior

The vertebral body models, intervertebral discs, and ligaments were assembled into spinal functional spinal units (FSU).

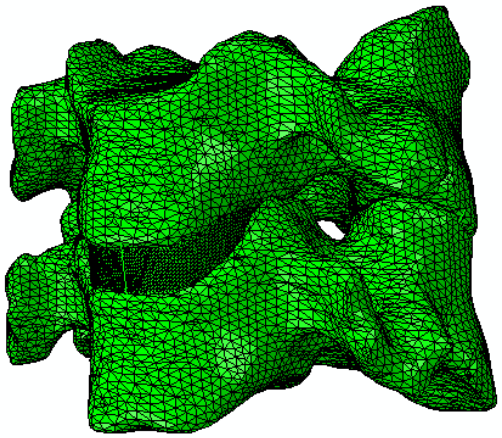

Figure 10. C3-C4 Functional Spinal Unit

Four two segment FSU were created included the C3-C7 vertebral levels. Each two segment FSU was validated under 1 Nm pure moments in flexion extension, bending, and axial rotation. The pure moments were applied to the superior vertebral body whilst the inferior endplate of the inferior vertebral body was fully fixed. The segment range of motion results were compared with in-vitro and finite element studies. The validated studies were subject to further analyses of their biomechanical behavior.

3.5 Cervical Spine Injury and Disease

The cervical spine region has higher range of motion as compared to other spine regions. The high levels of motion the cervical spine allows, leave it at a higher risk of injury as compared to the other spine regions. Soft tissue injuries such as ligament sprains and disc herniation can occur in the cervical spine. An injury to the cervical spine, in addition to other symptoms often presents with a reduction in ROM. Apart

from injury, there are various disease processes that can affect the cervical spine. Cervical spine intervertebral disc degeneration can occur with both the nucleus pulposus and annulus fibrosus regions losing their load bearing characteristics [21,22]. Disc degeneration can also present in disc herniation. Disc herniation involves the nucleus pulposus breaking its boundaries and pushing into the annulus region. This herniation causes pain in the disc and can have adverse effects on other regions of the spine. As stated, one of the primary functions of the spine is to protect the spinal cord. The spinal cord is extremely sensitive and can be damaged when a cervical spine injury occurs or when degenerative or congenital diseases such as spinal stenosis, myelopathy, and radiculopathy are present. These conditions are all indicative of some form of impingement on the spinal cord. Spine impingement can arise from herniation of the intervertebral discs into the spinal canal space, and or formation of bony osteophytes encroaching into the disc space to name a few disease processes [22,59-61]. Figure 13 illustrates some of these processes in a case of cervical radiculopathy via illustration and X-ray.

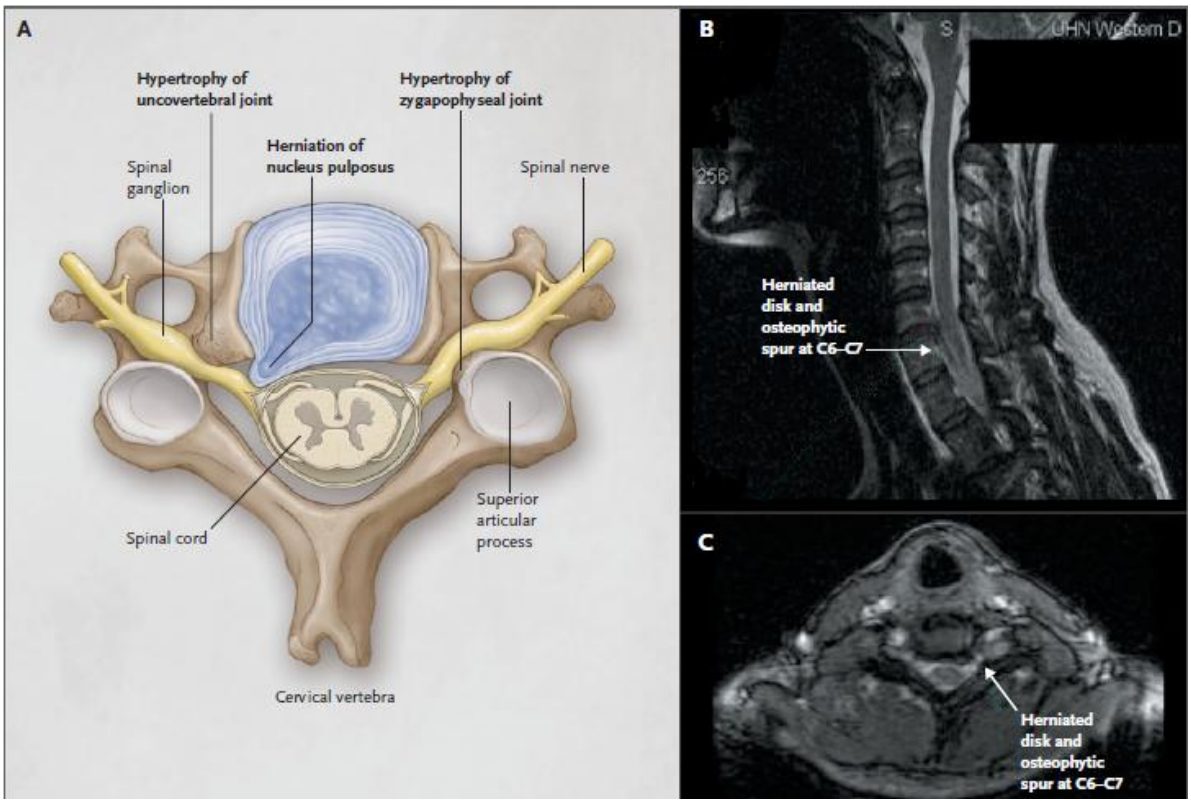

Figure 11. Cervical Radiculopathy [59]

Spine disorders such as disc degeneration and spinal stenosis can act as co morbidities. As such, interventions to address them are usually interrelated. A common treatment for intervertebral disc degeneration is the removal of the disc and fusion of the adjacent vertebral bodies. By removing the intervertebral disc, symptoms suffered can be alleviated, however the fusing of vertebral levels does limit spine ROM [16]. Spinal laminectomy and facetectomy are intervention options when faced with spine impingement by vertebral bony regions and joints. The procedures involve removing vertebral lamina and pedicles or facets [22]. In the case of cervical laminectomy, removal of the lamina and pedicle results in increased instability of the spinal segments.

The instability can be somewhat alleviated by performing a spinal fusion in concert or performing a cervical laminoplasty. Cervical laminoplasty involves removing a portion of the vertebral lamina thus preserving some stability [59,62]. Understanding some of the disease and injury processes, and interventions applied to the cervical spine can allow for further study using finite element modeling and analysis.

3.5.1 Disc Degeneration Simulation

In order to simulate degenerative disc disease in the upper cervical spine, the C3-C4 FSU was modified. Two grades of disc degeneration were considered, minor and moderate. The two grades were simulated by implementing changes to the mechanical properties of the discs [22,60,61].

Grade 1: The disk elastic modulus was increased to two times the elastic modulus of the disk annulus in the healthy model.

Grade 2: The disk modulus was increased to two times the modulus of the disk annulus in the healthy model. The elastic modulus of the disk annulus was increased to two times the value of the disk annulus in the healthy model. The annulus fiber volume was reduced by 25% from the value of the intact model.

The two grades of disc degeneration were analyzed in the C3-C4 FSU under 500 – 2500 Nmm of pure flexion and extension moments.

3.5.2 Cervical Laminectomy Simulation

As discussed, cervical laminectomy is a surgical option for treating spinal disorders or injury that are characterized by some form of spinal cord impingement. By removing vertebral lamina and pedicles spinal cord impingement can be relieved. In order to simulate a cervical laminectomy the cervical lamina and pedicles of the superior vertebral body in the two segment FSUs were removed along with the pertinent ligaments.

Chapter 4 – Results & Discussion

4.1 Model Validation

Each cervical FSU was validated under pure moment loads ranging from 1000 – 2500 Nmm. The measured ROM in each bending mode was compared to that of in-vitro and in some cases analytical FE studies. Results are presented for the 1000 Nmm moment loading showing the ROM for each FSU in Figures 12 - 15.

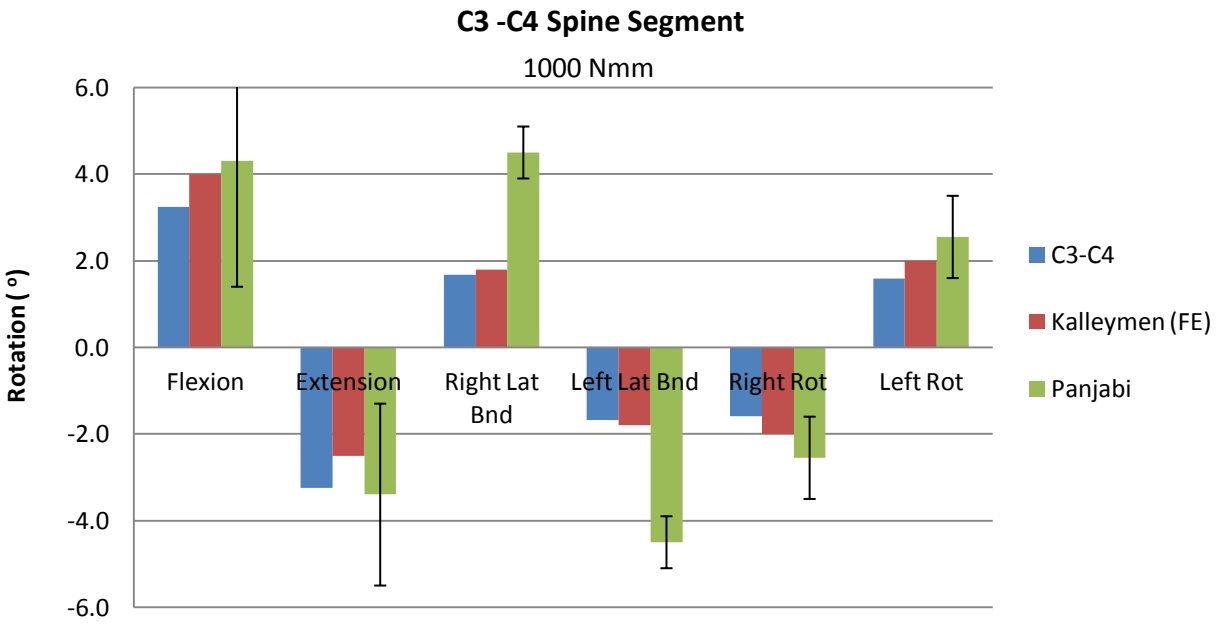

Figure 12. C3-C4 FSU Range of Motion

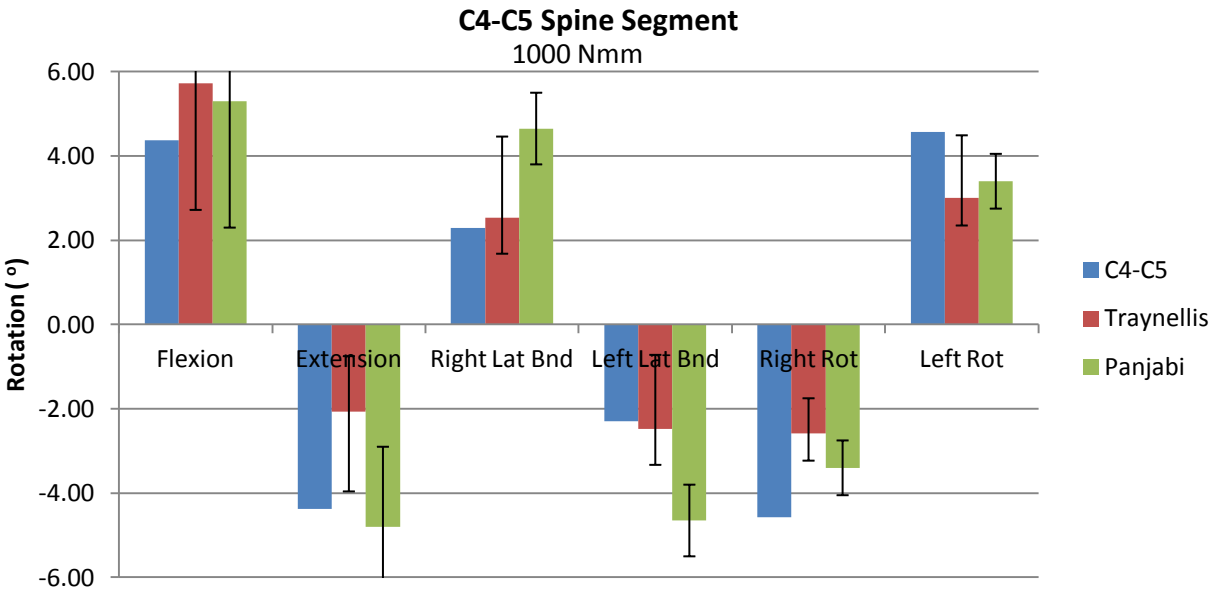

Figure 13. C4-C5 FSU Range of Motion

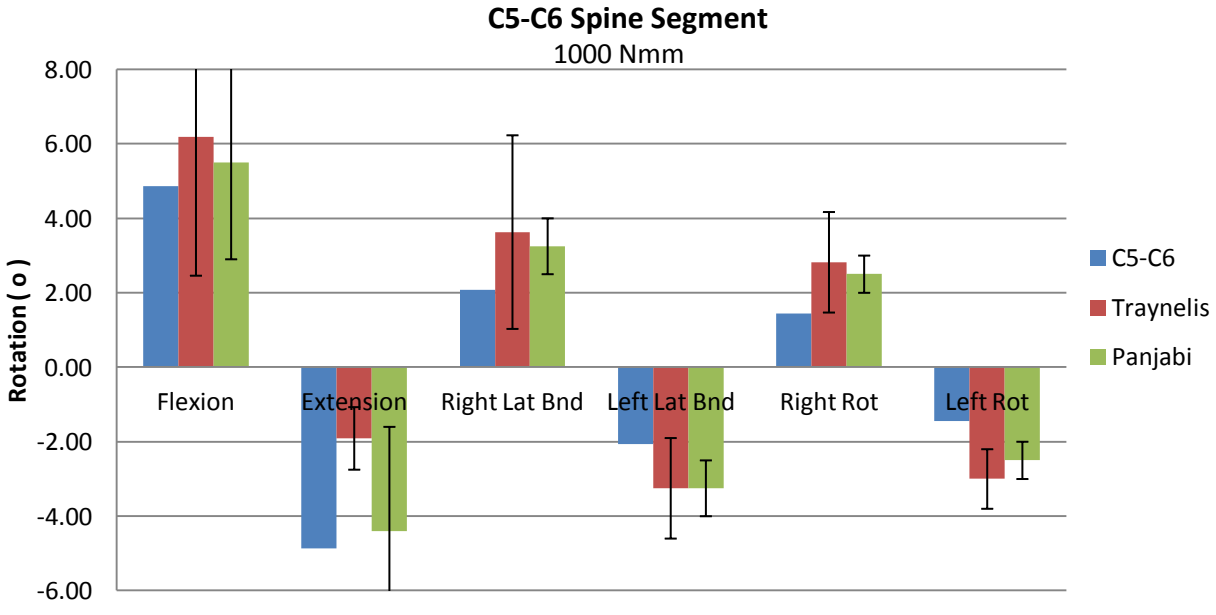

Figure 14. C5-C6 FSU Range of Motion

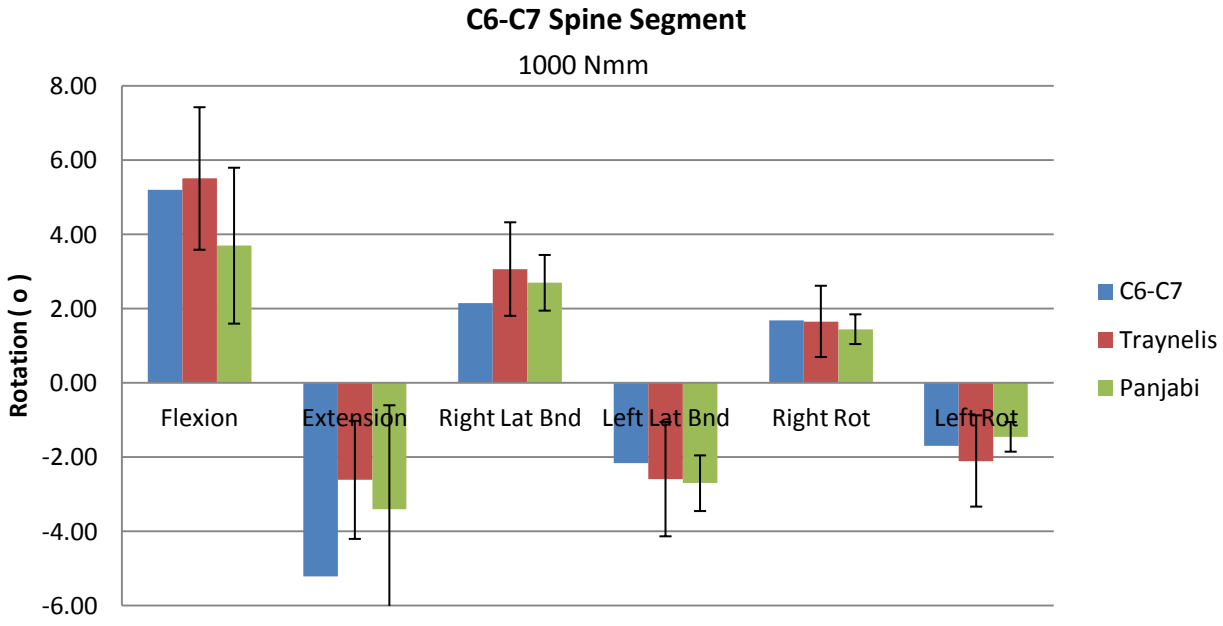

Figure 15. C6 – C7 FSU Range of Motion

The range of motion for all but the C3-C4 FSU in bending were within a standard deviation of in-vitro values. These results validate the finite element models and boundary conditions and loads applied to them. Taking a closer look at Figure 12, the C3-C4 FSU bending results shows that they clearly match the finite element analysis ROM found by Kallemeyn et al [9]. This agreement with a very recent finite element study validates the current C3-C4 FSU. It must also be noted that in some cases, including C4-C5 bending seen in Figure 13, the two in-vitro studies bending ROM are not in agreement. This illustrates that there can be a great deal of variability between different studies based on a myriad of factors. The validation of the cervical spine finite element model allows for its use in further studying cervical biomechanics and injury.

4.2 Disc Degeneration & Cervical Laminectomy

Disc degeneration was simulated in the C3-C4 FSU by applying changes to the intervertebral disc material properties as prescribed earlier. Pure moment loads ranging from 500 – 2500 Nmm pure moments were applied. The degenerated disc ROM were compared with that of the healthy disc and are reported for extension moments in Figure 16.

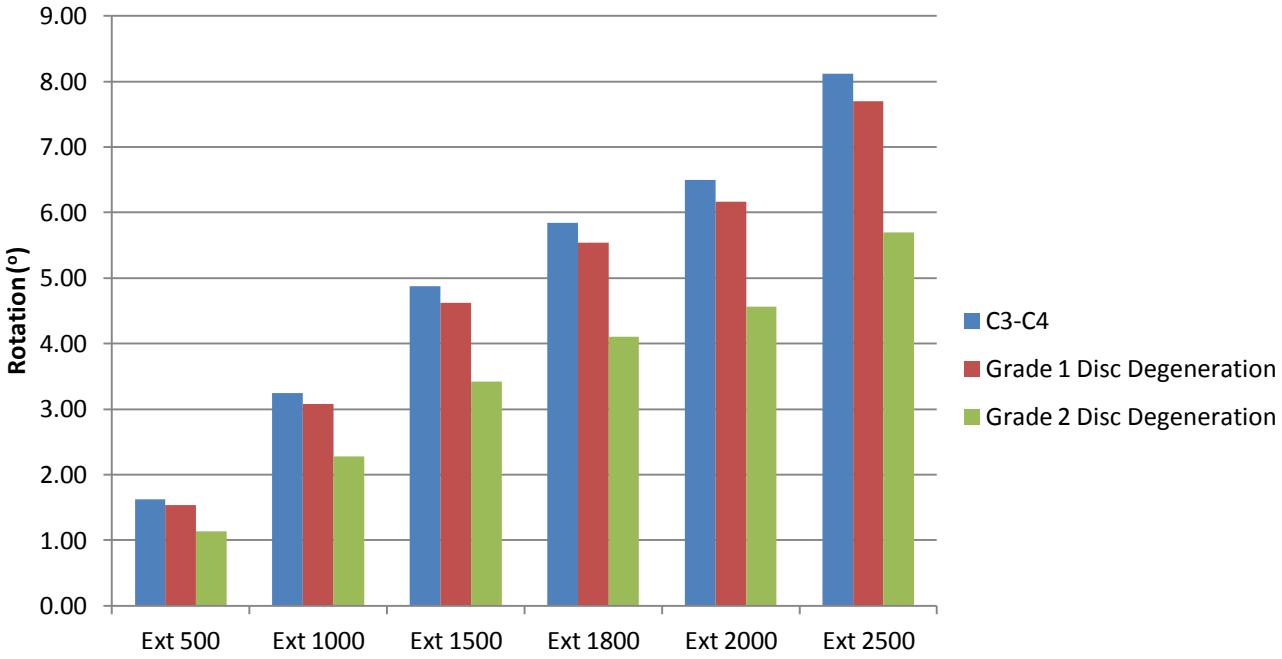

Figure 16. Disc Degeneration Range of Motion

The analysis results shown in Figure 16 illustrate that ROM decreased due to disc degeneration. The severity of the degeneration process also seems to play a role in the reduction in ROM as the grade 2 degenerated disc ROM is lower than both the healthy

and grade 1 degenerated disc. The results further echo what has been observed in disc degeneration cases.

Cervical laminectomy of the C3 vertebra was simulated as prescribed earlier. Pure moment loads were applied ranging from 500 – 2500 Nmm. The ROM results are presented along with the degenerated disc and healthy disc cases in Figure 17.

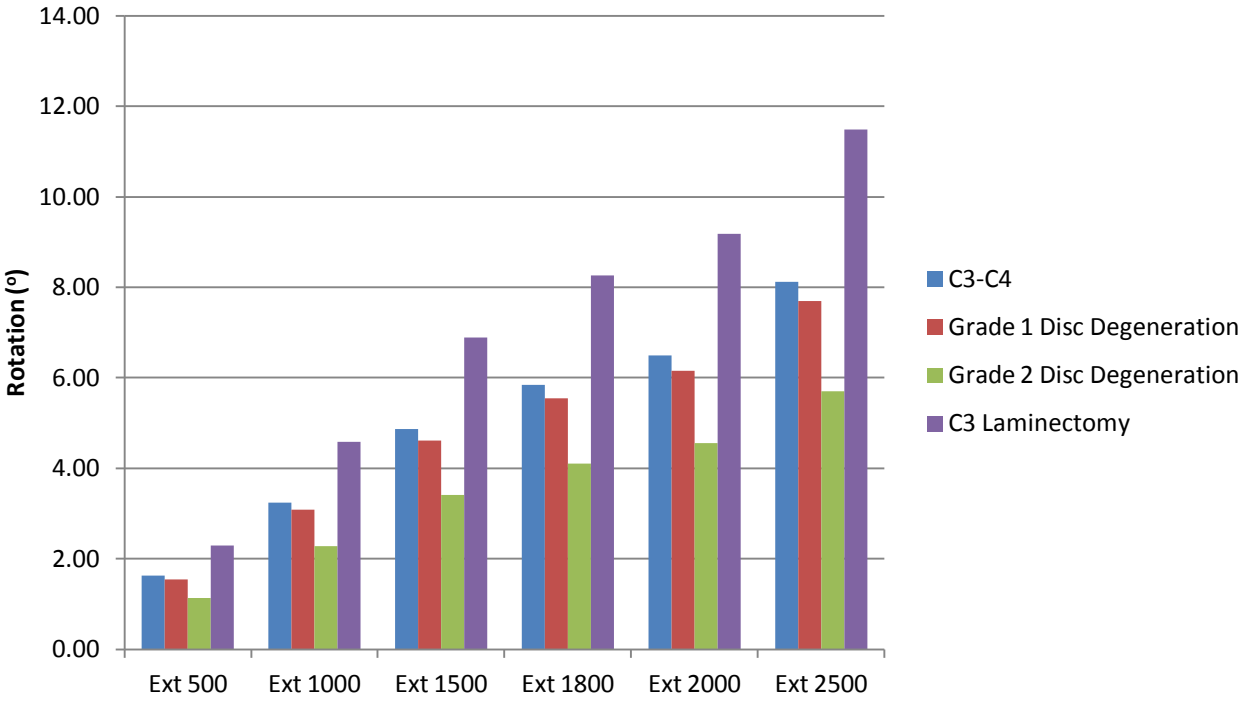

Figure 17. C3 Laminectomy Range of Motion

The results shown in Figure 17 reflect that cervical laminectomy introduces a level of instability to the FSU. This result is not surprising as laminectomy not only removes bony support structures from the FSU, but connective stabilizing ligaments including the ISL, and LF. In order to validate and better understand the significance of disc degeneration and cervical laminectomy on FSU ROM, a Monte Carlo analysis was

performed to increase the sample size of the available data. Means and standard deviation of the ROM for each case were input as bounding parameters for the simulation. The Monte Carlo was iterated 100 times to produce a data set of 30 ROM simulations. An analysis of variance (ANOVA) was performed on the expanded data set with a summary presented in Figure 18.

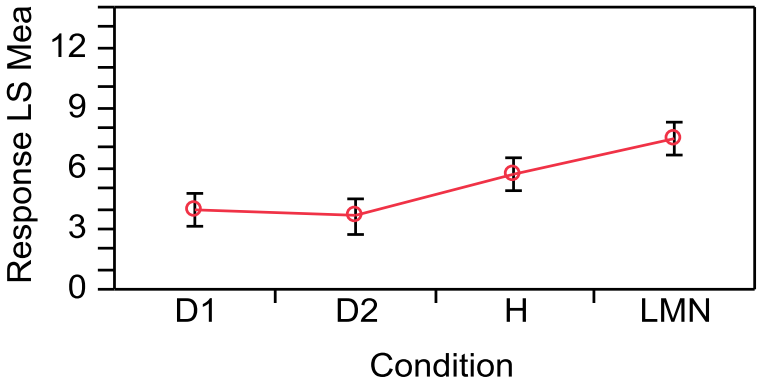

Level			Least Sq Mean
LMN	A		7.5093333
H		B	5.6866667
D1		C	3.9136667
D2		C	3.6253333

Levels not connected by same letter are significantly different.

Figure 18. Analysis of Variance

The ANOVA confirmed that the laminectomy and degenerated disc cases are significantly different from the healthy disc. Additionally, the ANOVA showed that laminectomy is significantly different from the disc degeneration cases. The study has confirmed that degenerative disease and surgical interventions have a clear impact on cervical spine biomechanics. The results were not unexpected as they reflect clinical

outcomes. Having a validated FE model that accurately reflects cervical spine biomechanics in healthy and diseased cases preserves a powerful tool for better understanding disease and injury mechanisms.

Chapter 5 – Cervical Spine Injury Risk

Cervical spine injuries can occur under a myriad of conditions. Injury mechanisms are difficult to quantify because deflections, stresses, and strains cannot be measured in-vivo during the event. Anthropometric test dummies (ATD) allow for in-vitro simulation of injury scenarios. ATDs are somewhat limited in their ability to accurately represent the behavior and response of the cervical spine. FE models can also be used for the study of cervical spine neck injury scenarios.The validated cervical spine FSUs were assembled along with the C2 vertebral body level and disc were assembled to create C2 – C7 spinal modelwhich is displayed in Figure 19. The model would be used to study cervical spine injury risk under dynamic loading conditions.

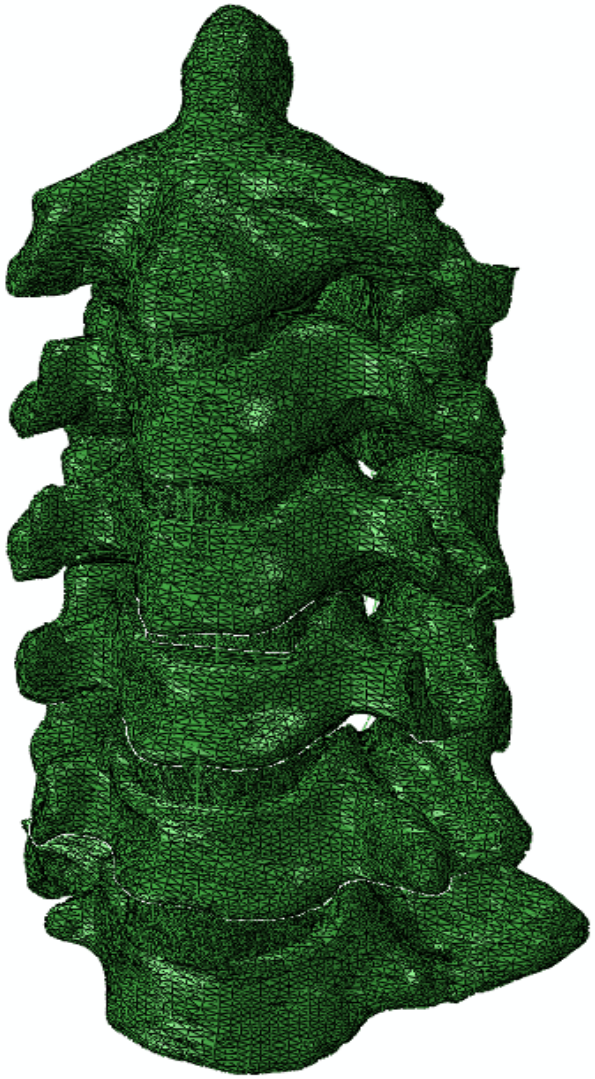

Figure 19. C2-C7 Cervical Spine Finite Element Model

5.1 Anti Vehicle Mine Detonation Simulation

The C2-C7 model was to be used to study the injury scenario of an anti vehicle mine exploding detonating under a vehicle. This scenario was modeled using ATD by Leerdam [63]. Occupants in a vehicle that experiences an anti vehicle mine detonation underneath are exposed to various loads. By simulating this scenario with and ATD, Leerdam was able to measure the axial compressive loads and durations the occupants are exposed to [63]. The blast response is made up of two components, local and global effects on vehicle passengers. Local effects pertain to the initial blast wave directly impacting vehicle occupants. Global effects represent the vehicles ensuing response to the reflecting blast wave in the form of a pressure force acting on occupants. Over about a 100 ms period each response was measured for various parts of the body. The load mechanisms and time periods along with the loads applied to the occupants are provided in Figures 20 – 22.

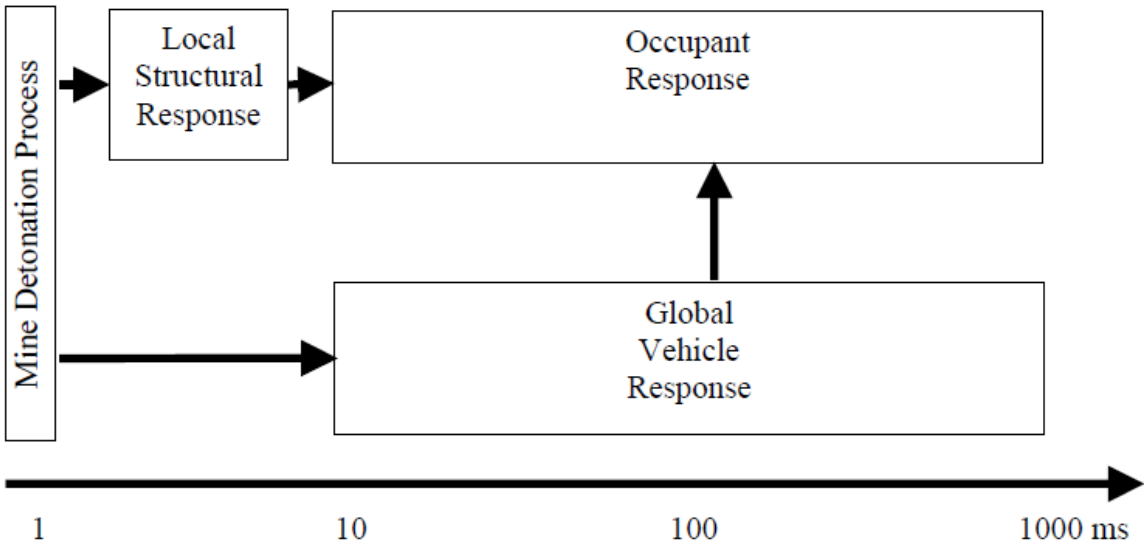

Figure 20. Anti Vehicle Mine Detonation Time Sequence [63]

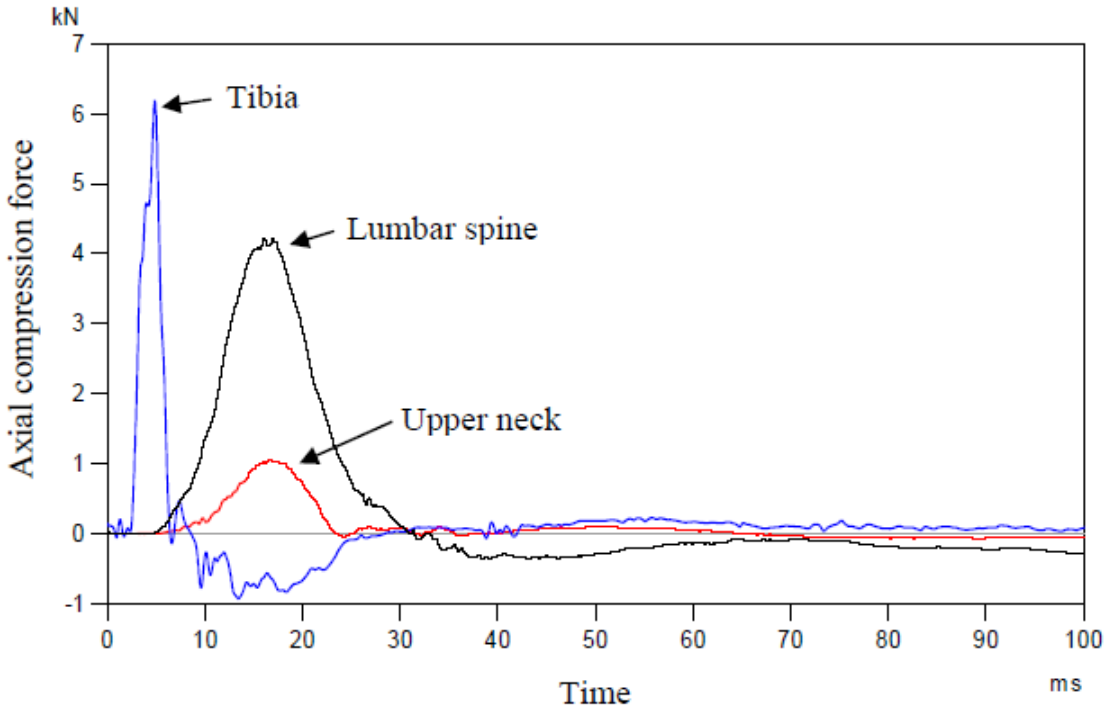

Figure 21. Local Detonation Effects [63]

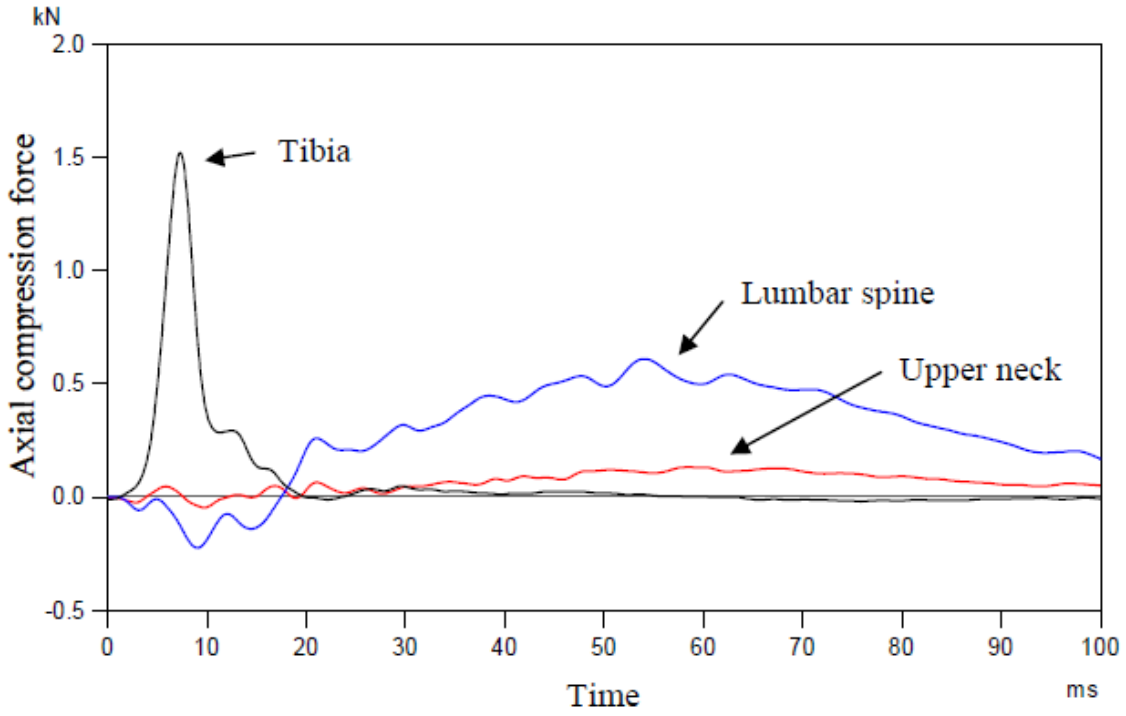

Figure 22. Global Detonation Effects [63]

These load scenarios were applied to the C2 – C7 cervical spine model. The load was applied to the superior surface of the C2 vertebra. The inferior endplate of the C7 vertebra was fully fixed in order to isolate the cervical region. In order to accommodate the dynamic load scenario, the intervertebral disc constitutive models were updated. A viscoelastic constitute model was employed because it offered better representation of the system under the dynamic load. The prior employed linear elastic constitutive model held well in the static domain but did not hold for the rapid dynamic load response in this scenario. The viscoelastic material property definitions were based on relaxation test data and material properties presented in Table 8. [17,58,64].

Table 8. Viscoelastic Intervertebral Disc Properties [17,58,64]

	Shear Relaxation Modulus (g_i)	Bulk Relaxation Modulus (k_i)	Relaxation Time Constant (τ_i)
Nucleus	0.638	0	0.141
E = 3.4 MPa	0.156	0	2.21
v = 0.49	0.12	0	39.9
ρ = 1.02e-6 Kg/mm^3	0.0383	0	266
	0	0	500
Annulus	0.399	0.399	3.45
E = 4.2 MPa	0	0.3	100
v = 0.45	0.361	0.149	1000
ρ = 1.05e-6 Kg/mm^3	0.108	0.15	5000

5.1.1 Results Summary

The blast mine simulation local and global axial compression force profiles were applied to the C2-C7 model. A dynamic analysis was completed. A summary of the blast mine simulation average intervertebral disc stressesis provided in Figure 23.

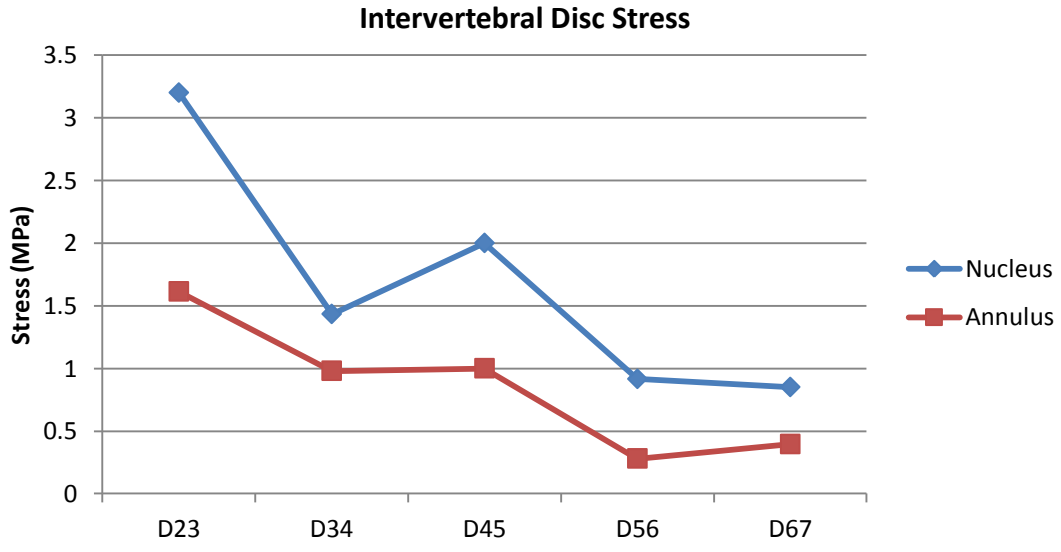

Figure 23. Anti Vehicle Blast Mine Disc Stresses

5.2 Injury Risk Assessment

Understanding the potential risk of injury to the cervical spine during various scenarios can aid in designing safety equipment or safety protocols to protect the spine. Cervical spine injury risk tolerance levels have been developed and studied with the use of ATDs. Mertz et al. developed an injury risk curve based on axial compressive forces applied over time on a 50^{th} percentile male Hybrid III ATD. The axial compressive forces measured on the Hybrid III ATD were considered representative of forces the human neck could experience under similar loads and durations [65,66]. The injury risk criteria displays regions within which the likelihood of a serious cervical spine injury due to compression may occur. The bottom threshold originates with a 4000 N compression force applied for 0 ms representing a remote risk of serious injury. The upper threshold originates with a 6670 N load applied instantaneously for presenting a potential risk for serious injury. Both slopes settle at a load of 1100 N representing a minimal risk of injury when applied for 30 ms, and representing a potential for serious injury when applied for 35 ms respectively [63]. The injury curves are shown in Figure 24 with the thresholds for different injury risk levels clearly visible.

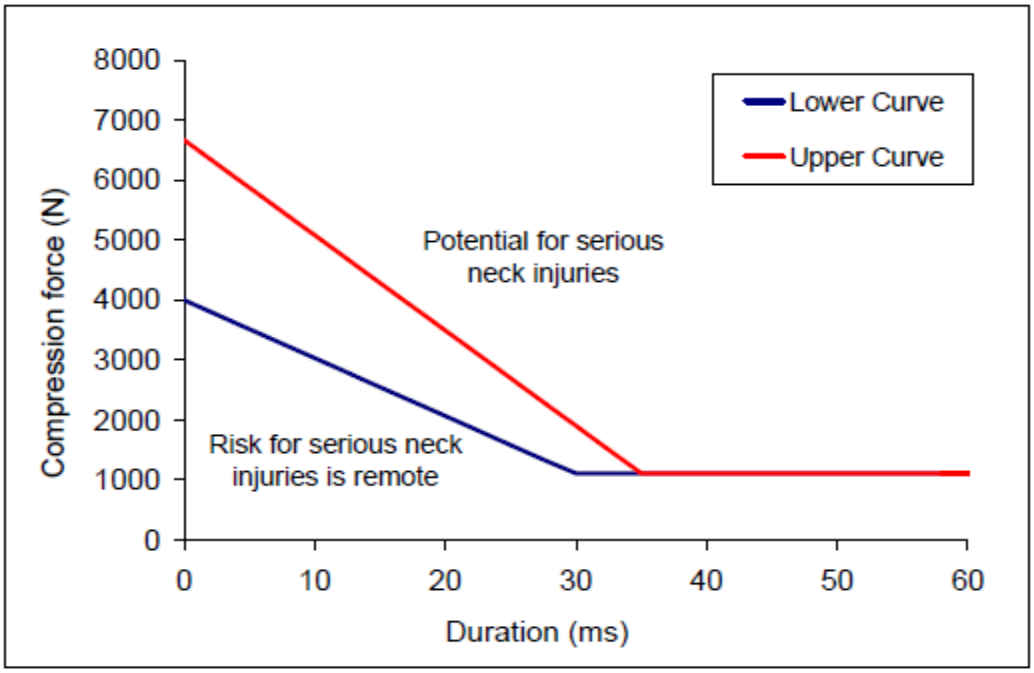

Figure 24. Compression Injury Risk Curve [63]

5.2.1 Anti Vehicle Blast Mine Injury Risk

Based on the anti vehicle mine blast profiles, the maximal load on the cervical spine is about 1000 N experienced for a period of about 10 ms. By applying 10 ms loads ranging from the origin of the minimal risk of injury threshold to exceeding the potential risk for serious injury threshold quantitative injury risk parameters can be estimated. Loads were applied from 3000 N to 6000 N for a duration of 10 ms to the C2-C7 model. Each load was assigned a risk of serious injury likelihood ranging from remote to very likely. Figure 25 illustrates the injury risk thresholds and the potential injury loads superimposed on the standard injury risk thresholds.

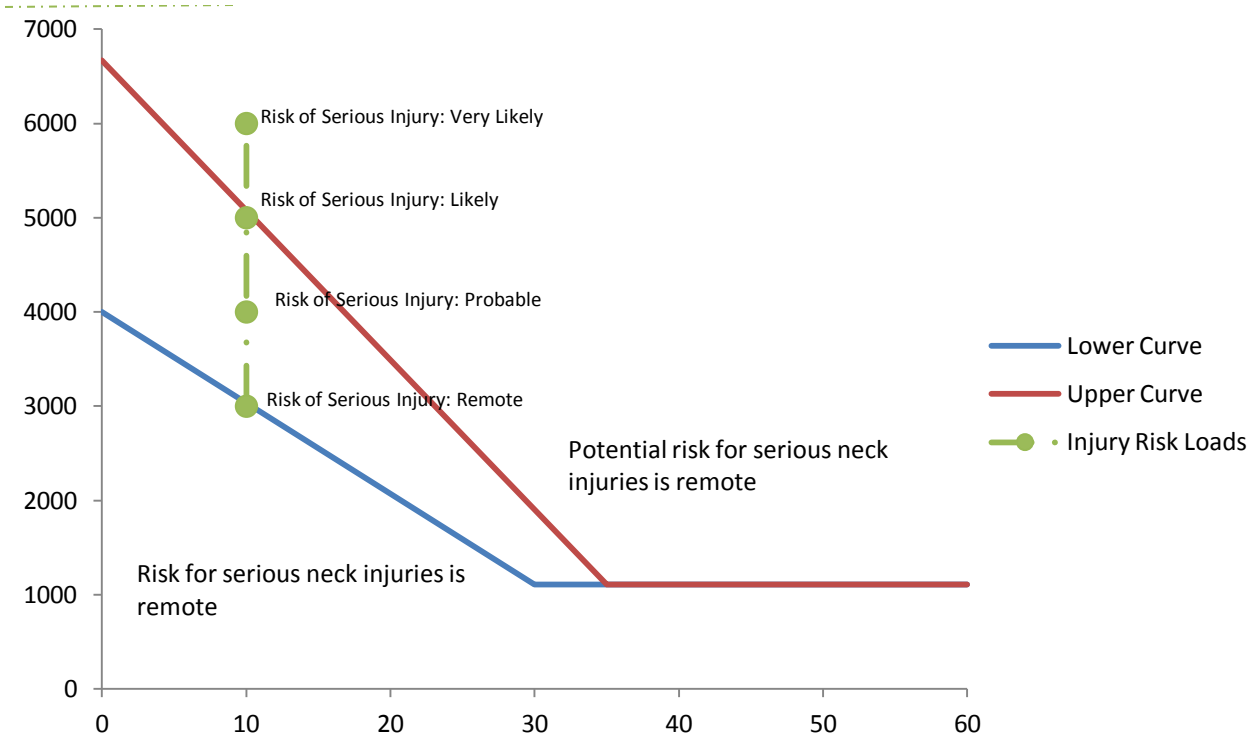

Figure 25. Injury Risk Curves & Loads [63]

Stress results for the nucleus and annulus regions of each disc were plotted for each load scenario. Results are presented in the following Figures 26 and 27.

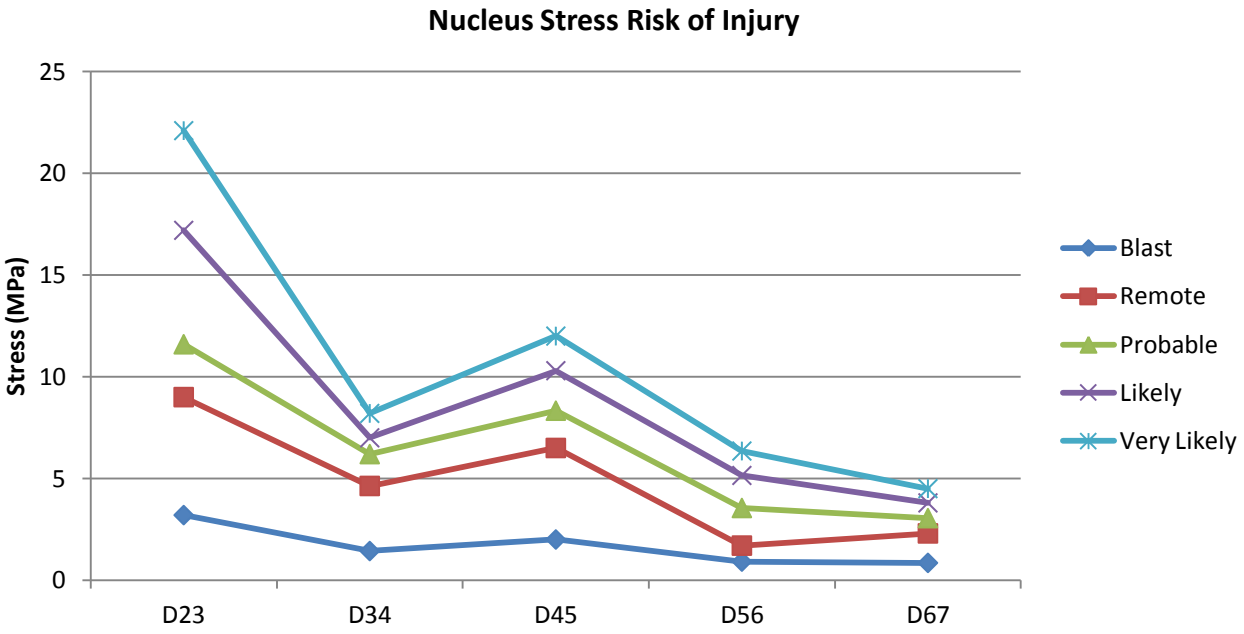

Figure 26. Nucleus Stresses

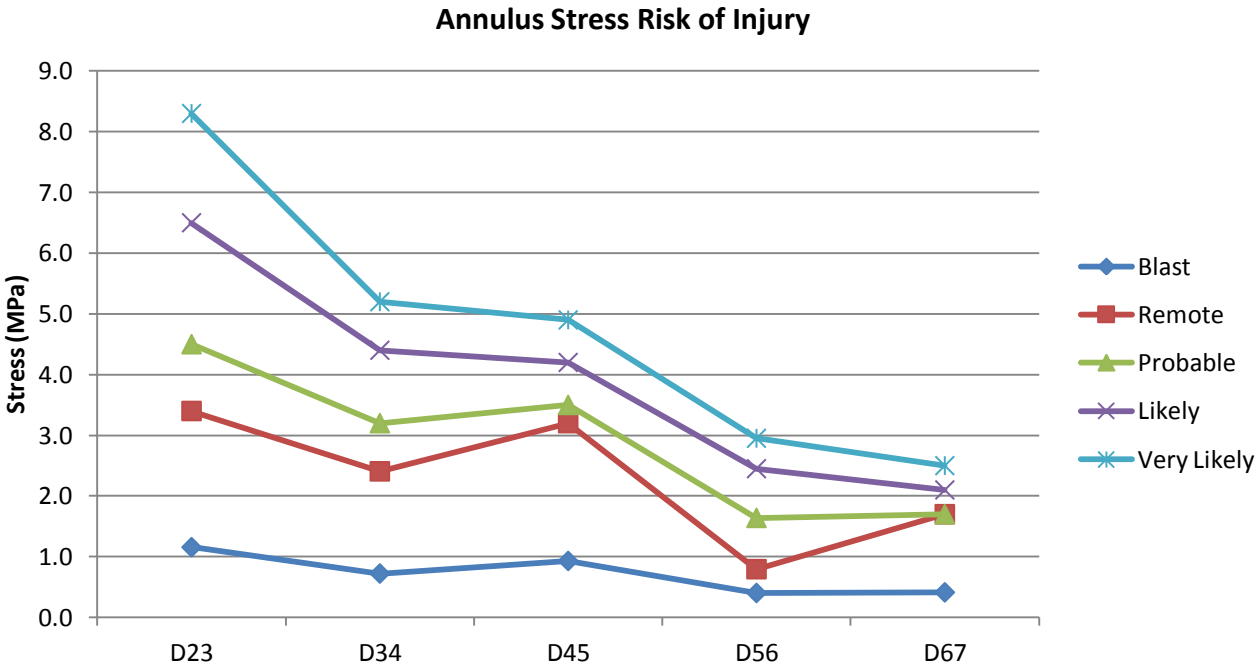

Figure 27. Annulus Stresses

The disc stress outputs indicate that the stress levels from the anti vehicle blast mine simulation do not exceed any of the stresses experienced at the prescribed injury

risk loads. This result is feasible as the maximal load applied during the blast is about 1000 N for a 10 ms period which is about 2000 N bellow the remote risk of injury threshold. It must be noted that the ATD derived injury risk criteria sets thresholds for risks of serious neck injury. This is not to say that the blast load did not cause some sort of minor injury to the intervertebral discs.

5.2.2 Injurious Disc Stress Prediction

The blast mine injury risk analysis has determined that according to the Leerdeman cervical spine compressive force duration injury risk curve, the blast does not pose significant risk of serious injury to the cervical spine. Using the data collected from the analysis, disc stress prediction models can be approximated. The disc stresses were measured at each disc level for the 3000 – 6000 N over a 10 ms duration loads. Considering each disc individually, the stress data can be curve fit in order to determine a stress prediction relationship. The following Figures, 28 – 32, display the stress data points for the annulus and nucleus regions along with the curve fit and expressions and R^2 values.

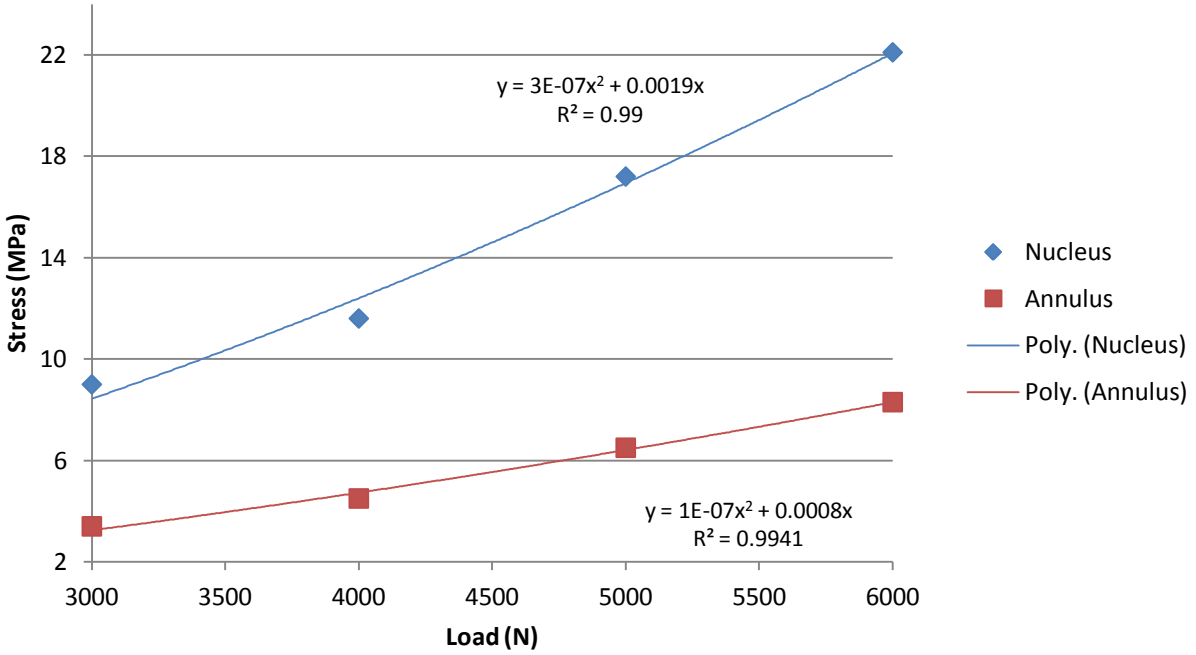

Figure 28. C2-C3 Disc Stress Curve Fit

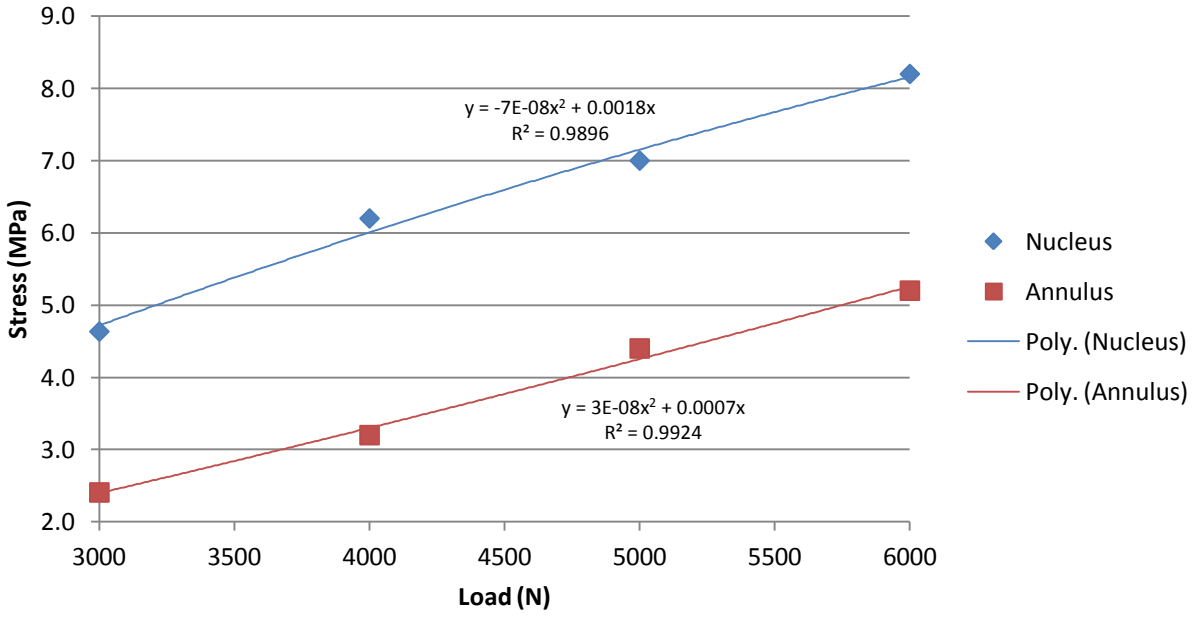

Figure 29. C3-C4 Disc Stress Curve Fit

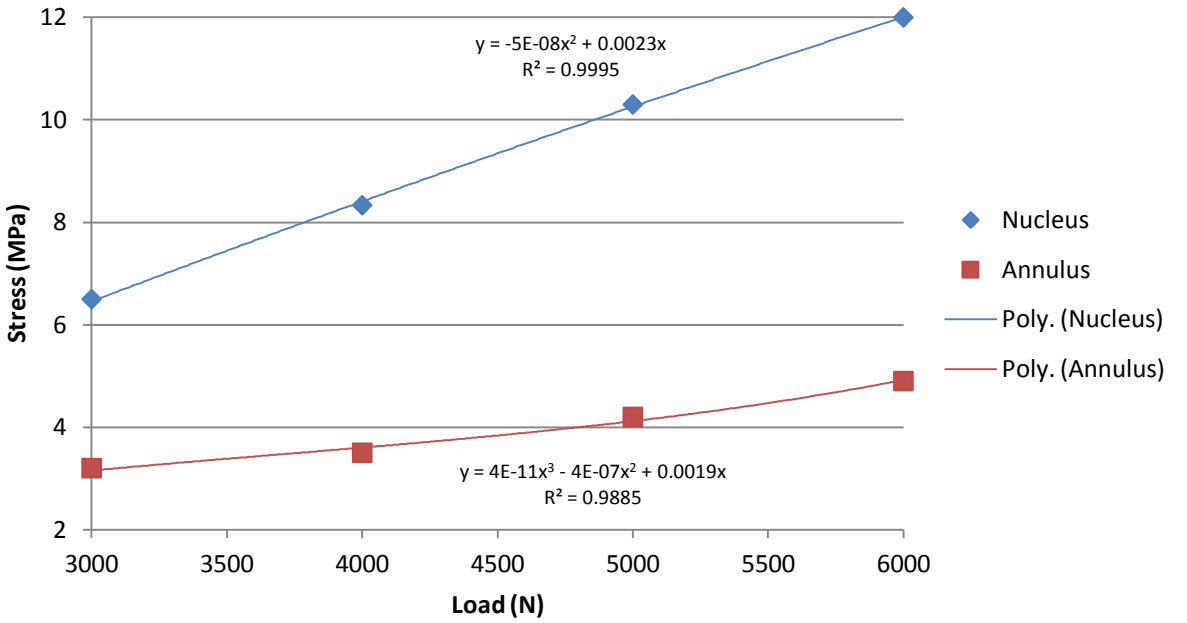

Figure 30. C4-C5 Disc Stress Curve Fit

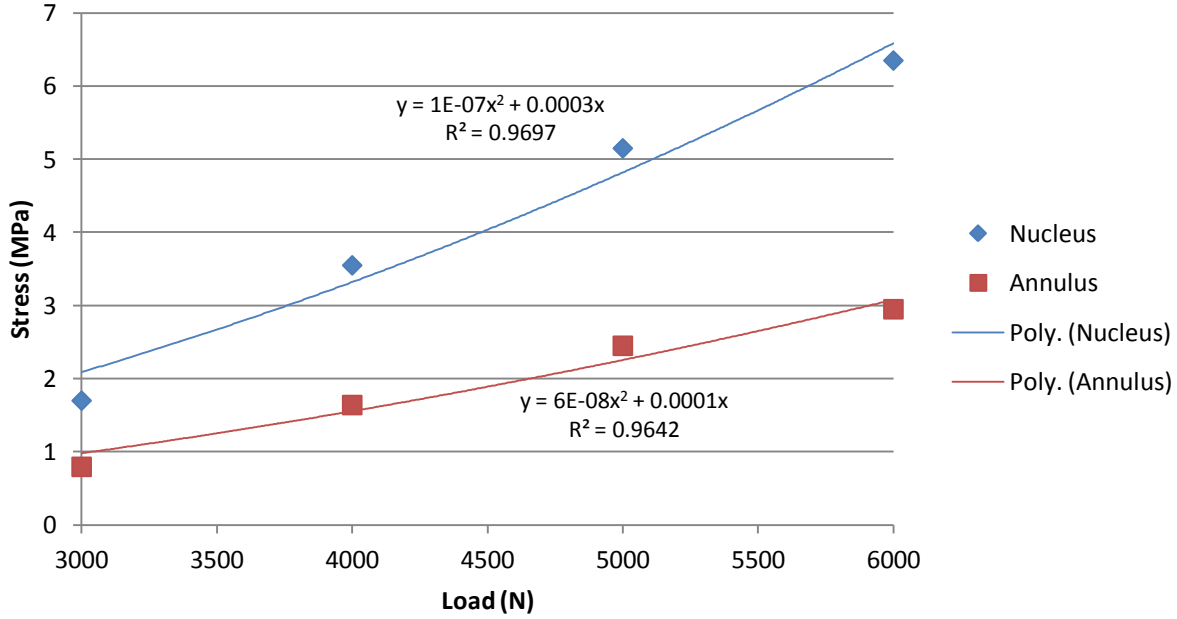

Figure 31. C5-C6 Disc Stress Curve Fit

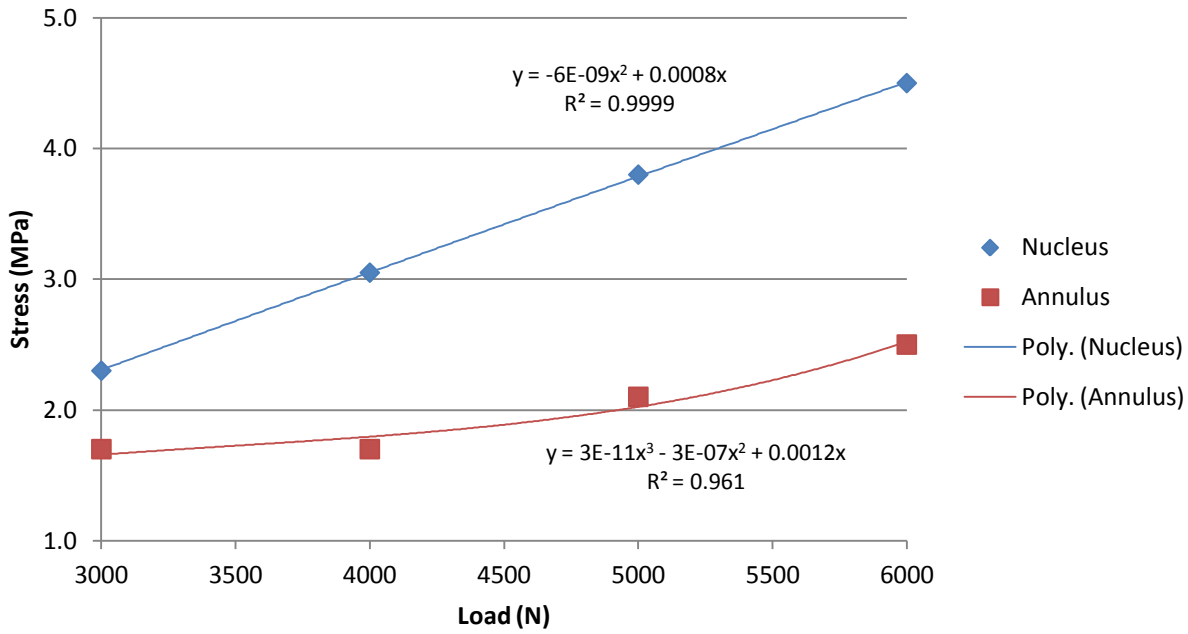

Figure 32. C6-C7 Disc Stress Curve Fit

A summary of the curve fit expressions and R^2 values are presented in Table 9. The curve fitting expressions were used to predict the disc stress resulting from the anti vehicle blast mine simulation; 1000 N for 10ms duration and are compared with the analytical results in Table 10.

Table 9. Disc Stress Prediction Expressions

Vertebral Level	Nucleus		Annulus	
	Expression	R^2	Expression	R^2
C2-C3	$y = 3E\text{-}07x^2 + 0.0019x$	0.99	$y = 1E\text{-}07x^2 + 0.0008x$	0.99
C3-C4	$y = -7E\text{-}08x^2 + 0.0018x$	0.99	$y = 3E\text{-}08x^2 + 0.0007x$	0.99
C4-C5	$y = -5E\text{-}08x^2 + 0.0023x$	0.99	$y = 4E\text{-}11x^3 - 4E\text{-}07x^2 + 0.0019x$	0.99
C5-C6	$y = 1E\text{-}07x^2 + 0.0003x$	0.97	$y = 6E\text{-}08x^2 + 0.0001x$	0.96
C6-C7	$y = -6E\text{-}09x^2 + 0.0008x$	0.99	$y = 3E\text{-}11x^3 - 3E\text{-}07x^2 + 0.0012x$	0.96

Table 10. Disc Stress Comparison

Vertebral Level	Nucleus Disc Stress (MPa)		Annulus Disc Stress (MPa)	
	Analysis	Predicted	Analysis	Predicted
C2-C3	2.7	2.2	1.2	0.9
C3-C4	1.6	1.7	0.7	0.7
C4-C5	1.7	2.3	0.9	1.5
C5-C6	0.9	0.4	0.4	0.2
C6-C7	0.8	0.8	0.4	0.9

The curve fit expressions seem to represent the analytical anti vehicle blast mine disc stresses well. The C4-C5 and C5-C6 showed the most discrepancies between the analytical and predicted stress values. The positive results are encouraging considering the small sample size of the measurements. The stress results can also be used to somewhat predict the risk of cervical spine injury based on apparent disc stress. Disc stresses corresponding to the Leerdeman cervical spine compressive loads, 3000 N – 6000 N, have been derived analytically and can be compared with apparent disc stresses derived from different axial load cases. For instance, for the C2-C3 level nucleus stresses of greater than about 20 MPa can indicate a high likelihood of serious injury. Figure 33 illustrates this injury risk prediction concept.

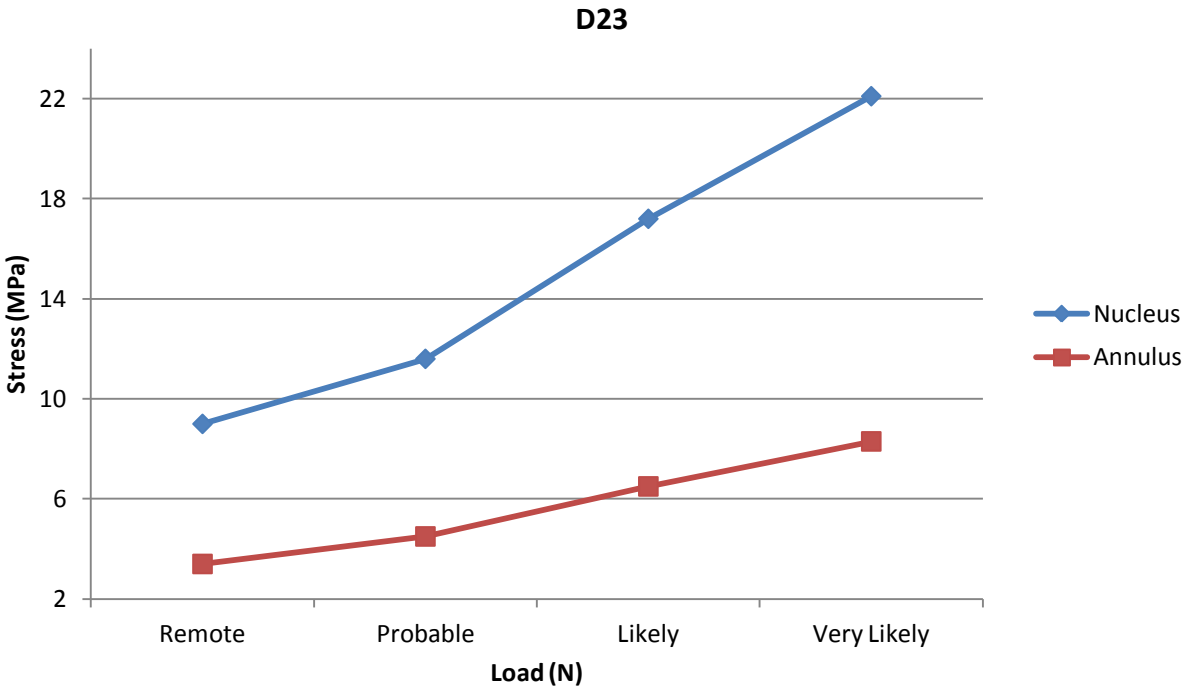

Figure 33. C23 Disc Stress Injury Risk

Chapter 6 – Conclusion

The study aimed to better understand cervical spine biomechanics and injury by developing a representative finite element model. The model was developed based on CT scans of a healthy adult male. The model functional spinal units were validatedagainst in-vitro studies for range of motion. The validated models were used to study cervical spine disease and injury. Multiple cases of disc degeneration and spinal laminectomy were performed. The analysis results correlated well with clinical findings of reduced cervical spine range of motion in cases of disc degeneration and increased instability due to laminectomy. The ability to run multiple injury and disease cases illustrates the advantages of employing finite element analysis in better understanding cervical spine behavior.

The validated cervical spine models were continually developed to create a C2-C7 cervical spine model. The model was applied to the study of cervical spine injury in the context of anti vehicle blast mine detonations. The study was performed to foster a better understanding of dynamic compressive loads on the neck and the risk of injury to the cervical spine. The analysis provided intervertebral disc stresses for each cervical spine level. The anti vehicle blast mine detonation compressive loads applied to the cervical spine were shown not to present significant risk of serious injury to the cervical

spine. This result fell in line with the fact the maximal blast mine detonation load for the 10ms duration was about 2000 N below the threshold for remote risk of serious injury. Data curve fitting was used to predict disc stresses at each vertebral level based on the axial compressive load applied. When compared with the blast mine detonation load of 1000 N over 10ms the prediction models showed very good agreement. The analytical stress results and prediction models create the groundwork for predicting the risk of serious cervical spine injury based on the Leerdeman injury risk curves and apparent disc stresses. This analysis continues to highlight the value of a finite element model of the cervical spine. It is clear that injurious loads cannot be applied to in-vivo studies of spine behavior. In-vitro analyses can be used to study injurious loads at the cost of the specimens. Furthermore, in-vitro analyses lack the capacity to report internal stress profiles.

The study fulfilled each of the goals prescribed. A validated model of the cervical spine was developed and applied to study injury and biomechanical behavior. The model was further developed to study injury risk in a dynamic load scenario and to better understand injury risk.

Chapter 7 – References

1. Leeardam P.J., Test Methodology for Protection of Vehicle Occupants against Anti-Vehicluar Landmine Effects, RTO Technical Report (2007) 3; 1-34

2. Ng, H.W.,Teo E.C., Nonlinear Finite-Element Analysis of the Lower Cervical Spine (C4-C6) Under Axial Loading, Journal of Spinal Disorders, (2001)14; 201-210

3. Panagiotopoulou O., Finite element analysis (FEA): applying an engineering method to functional morphology in anthropology and human biology, Annals of Human Biology, (2009) 36; 609-623

4. Yoganandan N., Kumaresan S., Voo L., Pintar FA., Finite elemnt applications in human cervical spine modeling, Spine (1996) 21; 1824-1834

5. Pitzen T., Geisler F., Matthis D., Muller-Storz H., Barbier D., Steudel W.I., Feldges A., A finite element model for predicting the biomechanical behaviour of the human lumbar spine, Control Engineering Practice (2002) 10; 83-90

6. Pitzen T., Matthis D., Steudel W.I., Posterior Element Injury and Cervical Spine Flexibility Following Anterior Cervical Fusion and Plating, European Journal of Trauma (2002) 28; 24-30

7. Bogduck N., Yoganandan N., Biomechanics of the cervical spine Part 3: minor injuries, Clinical Biomechanic, (2001) 16; 267-275

8. Yoganandan N., Kumaresan S., Pintar F.A., Biomechanics of the cervical spine part 2. Cervical spine soft tissue responses and biomechanical modeling, Clinical Biomechanics (2001) 16; 1-27

9. Kallemeyn N. A., Tadepalli S.C., Shivanna, K.H., An interactive multiblock approach to meshing the spine, Computer Methods and Programs in Biomedicine (2009) 95; 227-235

10. ZhangQ.H., Teo E.C., Ng H.W., Lee V.S., Finite element analysis of moment-rotation relationships for human cervical spine, Journal of Biomechanics (2006) 39; 189-193

11. Esat V., Lopik D., Acar M., Combined Multi-Body Dynamic and FE Models of Human Head and Neck, IUTAM Proceedings on Impact Biomechanics (2005) 91-100

12. Haghpanahi M., Mapar R., Development of a Parametric Finite Element Model of Lower Cervical Spine in Sagital Plan, Proceedings of the 28th IEEE EMBS Annual International Conference (2006) 1739-1741

13. Panzer M.B., Cronin D.S., C4-C5 segment finite element model development, validation, and load-sharing investigation, Journal of Biomechanics(2009) 42; 480-490

14. Bozkus H., Karakas A., Hanci M., Uzan M., Bozdag E., Sarioglu A., Finite element model of the Jefferson fracture: comparison with a cadaver model, European Spine Journal (2001) 10; 257-263

15. Teo J.C.M., Chui C.K., Wang Z.L., Ong S.H., Yan C.H., Wang S.C., Wong H.K., Teoh S.H., Heterogenous meshing and biomechanical modeling of human spine, Medical Engineering and Physics (2007) 29; 277-290

16. Li Y., LewisG., Influence of surgical treatment for disc degeneration diseases at C5-C6 on changes in some biomechanical parameters of the cervical spine, Medical Engineering & Physics (2010) 32; 593-503

17. Esat V., Acar M., Viscoelastic finite element analysis of the cervical inervertebral discs in conjunction with a multi-body dynamic model of the human head and neck, Journal of Engineering in Medicine (2009) 223; 249-262

18. Galbusera F., Bellini C.M., Raimondi M.T., Fornari M., Assietti R., Cervical spine biomechanics following implantation of a disc prosthesis, Medical Engineering and Physics (2008) 30; 1127-1133

19. Greaves C.Y., Gadala M.S., Oxland T.R., A three-dimensional finite element model of the cervical spine with spinal cord: an investigation of three injury mechanisms, Annals of Biomedical Engineering (2008) 36; 396-405

20. Wheeldon J.A., StempterB.D., Yoganandan N., Pintar F.A., Validation of finite element model of the young normal lower cervical spine, Annals of Biomedical Engineering (2008) 36; 1458-1469

21. Ha S.K., Finite element modeling of multi-level cervical spinal segments (C3-C6) and biomechanical analysis of an elastomer-type prosthetic disc, Medical Engineering & Physics (2006) 28; 534-541

22. NgH.W., Teo E.C., Zhang Q., Influence of Cervical Disc Degeneration after Posterior Surgical Techniques in Combined Flexion-Extension -- A Nonlinear Analytical Study, Journal of Biomechanical Engineering (2005) 127; 186-192

23. Brolin K., Halldin, P., Development of a Finite Element Model of the Upper Cervical Spine and a Parameter Study of Ligament Characteristics, Spine (2004) 29; 376-385

24. Ng H.W., Teo E.C., Lee K.K., Qiu T.X., Finite element analysis of cervical spinal instability under physiologic loading, Journal of Spinal Disorders & Techniques (2003) 16; 55-63

25. Teo E.C., Ng, H.W., First cervical vertebra (atlas) fracture mechanism studies using finite element method, Journal of Biomechanics (2001) 34; 13-21

26. Graham R.S., Oberlander E.K., Stewart J.E., Griffiths D.J., Validation and use of a finite element model of C-2 for determination of stress and fracture patterns of anterior odontoid loads, Journal of Neurosurgery (2000) 93; 117-125

27. Kumaresan S., Yoganandan N., Pintar F.A., Biomechanical study of pediatric human cervical spine: a finite element approach, Journal of Biomechanical Engineering(2000) 122; 60-71

28. Zheng N., Young-Hing K., Watson L.G., Morphological and biomechanical studies of pedicle screw fixation for the lower cervical spine, Journal of Systems Integration(2000) 10; 55-66

29. Kumaresan S., Yoganandan J., Pintar F., Maiman D., Finite element modeling of the lower cervical spine: role of intervertebral disc under axial and eccentric loads, Medical Engineering & Physics (1999) 21; 689-700

30. Kumaresan S., Yoganandan N., Pintar F., Finite Element Analysis of the Cervical Spine: A Material Property Sensitivity Study, Clinical Biomechanics (1999) 14; 41-53

31. Goel V.K., Clausen J.D., Prediction of Load Sharing Among Spinal Components of a C5-C6 Motion Segment Using the Finite Element Approach, Spine (1998) 23; 684-691

32. Yoganandan N., Kumaresan S., Voo L., Finite Element Analysis of the Human Lower Cervical Spine: parametric analysis of the C4-C6 unit, Journal of Biomechanics (1998) 119; 87-92

33. Maurel N., Lavaste F., Skalli W., A three-dimensional parameterized finite element model of the lower cervical spine. Study of the influence of the posterior articular facets, Journal of Biomechanics (1997) 30; 921-931

34. Voo L.M., Kumaresan S., Yoganandan N., Pintar, F.A., Cusik J.F., Finite element analysis of cervical facetectomy, Spine (1997) 22;964-969

35. Bozic K.J., Keyak J.H., Skinner H.B., Bueff H.U., Bradford D.S., Three-dimensional finite element modeling of a cervical vertebra: An investigation of burst fracture mechanism, Journal of Spinal Disorders (1994) 7; 102-110

36. Yoganandan N., Kumaresan S., Voo L., Pintar F., Finite Element Model of the Human Lower Cervical Spine: Parametric Analysis of the C4-C6 Unit, Journal of Biomechanical Engineering (1997) 119; 81-92

37. Ambard D., Cherblanc F., Mechanical Behavior of Annulus Fibrosus: A Microstructural Model of Fibers Reorientation, Annals of Biomedical Engineering (2009) 37; 2256-2265

38. Noailly J., Lacoix D., Planell J.A., Finite element study of a novel intervertebral disc substitute, Spine (2005) 30; 2257-2264

39. Coventry M.B., Ghormley R.K., Kernohan J.W., The intervertebral disc: its microscopic anatomy and pathology. Part II: Changes in the intervertebral disc concomitant with age, Journal of Boint and Joint Surgery (1945) 27; 233-247

40. Meakin J.R., Huskins D.W.L., Replacing the nucleus pulposus of the intervertebral disk: prediction of suitable properties of a replacement material using finite element analysis, Journal of Materials Science (2001) 12; 207-213

41. Eberlein R., Holzapfel G.A., FroelichM., Multi-segment FEA of the human lumbar spine including the heterogeneity of the annulus fibrosus, Computational Mechanics (2004) 34; 147-163

42. Palomar A., Calvo B., Doblare M., An accurate finite element model of the cervical spine under quasi-static loading, Journal of Biomechanics (2008) 41; 523-531

43. Schmidt H., Heuer F., Drumm J., Klezl Z., Claes L., Wilke H.J., Application of a calibration method provides more realistic results for a finite element model of a lumbar spinal segment, Clinical Biomechanics (2007) 22; 377-384

44. Yoganandan N., Kumaresan S., Voo L., Pintar F., Finite Element Analysis of the C4-C6 Cervical Spine Unit, Medical Engineering & Physics (1996) 18; 569-574

45. Ebara S., Iatridis J.C., Setton L.A., Foster R.J., Mow V.C., Weidenbaum M., Tensile properties of nondegenerate human lumbar annulus fibrosus, Spine (1996) 21; 452-461

46. Holzapfel, G A. Nonlinear Solid Mechanics, New York : Wiley, 2000

47. Yoganandan N., Kumaresan S., Pintar F.A., Geometric and mechanical properties of human cervical spine ligaments, Journal of Biomechanical Engineering (2000) 122; 623-629.

48. Brolin K., Halldin P., Leijonhufvud I., The effect of muscle activation on neck response, Traffic Injury Prevention (2005) 6; 67-76

49. Brolin K., Halldin P., Development of a finite element model of the upper cervical spine and a parameter study of ligament characteristics, Spine (2004) 29; 376-385

50. Stemper B.D., Yoganandan N., Pintar F.A., Rao R.D., Anterior longitudinal ligament injuries in whiplash may lead to cervical instability, Medical Engineering & Physics (2006) 28; 515-524

51. Noailly J., Wilke H.J., Planell J.A., Lacroix D., How does the geometry affect the internal biomechanics of a lumbar spine bi-segment finite element model? Consequences on validation process, Journal of Biomechanics (2007) 40; 2414-2425

52. Wheeldon J.A., Pintar F.A., Knowles S., Yoganandan N., Experimental flexion/extension data corridors for validation of finite element models of the young, normal cervical spine, Journal of Biomechanics (2006) 39; 375-380

53. Panjabi M.M., Crisco J.J., Vasavada A., Oda T., Cholewicki J., Nibu K., Shin E., Mechanical properties of the human cervical spine as shown by three-dimensional load-displacement curves, Spine (2001) 26; 2692-2700

54. Moroney S.P., Schultz A.B., Miller J.A., Andersson G.B., Load-displacement properties of lower cervical spine motion segments, Journal of Biomechanics (1988) 21; 769-779

55. Richter M., Wilke H.J., Kluger P., Claes L., Puhl W., Load-displacement properties of the normal and injured lower cervical spine in vitro, European Spine Journal (2000) 9; 104-108

56. Wilke H.J., Claes L., Schmitt H., Wolf S., A universal spine tester for in vitro experiments with muscle force simulation, European Spine Journal(1994) 3; 91-97

57. Bozkus H., Karakas A., Hanci M., Uzan M., Bozdag E., Sarioglu A.C., Finite element model of the Jefferson fracture: comparison with a cadaver model, European Spine Journal (2001)10; 257-263

58. Goel V.K., Park H., Kong W., Investigation of vibration characteristics of the ligamentous lumbar spine using the finite element approach, Journal of Biomechanical Engineering (1994) 116; 377-383

59. Carette S., Phil M., Fehlings M.G., Cevical Radiculopathy, New England Journal of Medicine (2008) 353; 392-399

60. Kumaresan S., Yoganandan N., Pintar F.A., Maiman D.J., Goel V.K., Contribution of Disc Degeneratation to Osteophyte Formation in the Cervical Spine: A Biomechanical Investigation, Journal of Orthopedic Research (2001) 19; 977-984

61. Lestini W.F., Wiesel S.W., The Pathogenesis of Cervical Spondylosis, Clinical Orthopedics (1989) 239; 69-93

62. Ullrich, P.F., Posterior Cervical Laminectomy, Spine Health. November 6, 2005; 1-7 http://www.spine-health.com/print/treatment/back-surgery/posterior-cervical-laminectomy

63. Leerdam P.J.C., Research experiences on vehicle mine protection, First European Survivability Workshop (2002)

64. Wang J.L., Parnianpour M., Shirazi-Adl A., Engin A.E., Viscoelastic finite-element analysis of a lumbar motion segment in combined compression and sagital flexion, Spine (2000) 25; 310-318

65. Mertz H.J., Hodgson V.R., Thomas L.M. Nyquist G.W., An Assessment of Compressive Neck Loads Under Injury-Producing Conditions, The Physician and Sport Medicine (1978) 6: 95-106

66. Mertz H.J.,Injury Assessment Values Used to Evaluate Hybrid III Response Measurements, Comment to the National Highway Traffic Safety Administration concerning Federal Motor Vehicle Safety Standard 208, Occupant Crash Protection. Enclosure 2 of Attachment 1 of Part III NHTSA (1984) Docket Document No. 74-14-N32-1666B

Chapter 8 – Appendix

8.1 Finite Element Model Details

Table 11. C2-C3 FE Model Details

	Element Type	Elements	Nodes
C2	S3	12548	28635
	C3D4	146385	
C3	S3	10756	20383
	C3D4	101636	
Disc	S3	N/A	7614
	C3D4	36991	
Ligaments	B31	15	20

Table 12. C3-C4 FE Model Details

	Element Type	Elements	Nodes
C3	S3	10756	20383
	C3D4	101636	
C4	S3	10528	19793
	C3D4	98070	
Disc	S3	4142	19236
	C3D4	64463	
Ligaments	B31	7	14

Table 13. C4-C5 FE Model Details

	Element Type	Elements	Nodes
C4	S3	10245	19145
	C3D4	104867	
C5	S3	10434	19401
	C3D4	95856	
Disc	S3	2438	5533
	C3D4	18575	
Ligaments	B31	22	29

Table 14. C5-C6 FE Model Details

	Element Type	Elements	Nodes
C5	S3	10171	8379
	C3D4	29678	
C6	S3	12432	9733
	C3D4	34276	
Disc 5_6	S3, S3R	6791	15710
	C3D4, C3D8R	52566	
Ligaments	B31	91	98

Table 15. C6-C7 FE Model Details

	Element Type	Elements	Nodes
C6	S3	12432	9733
	C3D4	34276	
C7	S3	11841	10294
	C3D4	37345	
Disc	C3D4	5149	1502
Ligaments	B31	74	81